To the Graduate Council:

I am submitting herewith a thesis written by Christine Hshiao-Mean Wu entitled "Pig Brain Pyridoxal Kinase and Pyridoxine-5-Phosphate Oxidase." I recommend that it be accepted in partial fulfillment of the requirements for the degree of Master of Science, with a major in Biochemistry.

Jorge E. Churchich, Major Professor

We have read this thesis
and recommend its acceptance:

Robert H. Tinberg

G. G. Joshi

Accepted for the Council:

L. Evans Roth
Vice Chancellor
Graduate Studies and Research

PIG BRAIN PYRIDOXAL KINASE AND PYRIDOXINE-5-PHOSPHATE OXIDASE

A Thesis

Presented for the

Master of Science

Degree

The University of Tennessee, Knoxville

Christine Hshiao-Mean Wu

June 1981

ACKNOWLEDGMENTS

The author wishes to express her fond appreciation to Dr. Jorge E. Churchich for his encouragement, advice and guidance throughout the pursuit of this degree. She wishes to thank her parents for offering her the opportunity to complete her studies in the United States.

She also wishes to thank her fellow graduate students, Mr. Sean Sullivan and Mr. Doo Sik Kim for their many practical suggestions, invaluable friendship and help. Her special appreciation goes to Dr. Anthony Huang for his kind corrections and suggestions in the rough draft of this thesis.

Finally, she would also like to thank Dr. R. H. Feinberg and Dr. J. G. Joshi for their valuable time to save on her examination committee.

ABSTRACT

The inhibition kinetic patterns obtained when ATP and pyridoxal analogues are used as inhibitors of the reaction catalyzed by pyridoxal kinase are consistent with a rapid equilibrium random Bi-Bi, in which binary complexes, i.e., enzyme-ATP and enzyme-pyridoxal, are formed in kinetically significant amounts. Protein fluorescence quenching was used to determine the dissociation constant (K_D = 25μM) of ATP-Zn bound to the nucleotide site of the kinase. The binding of ATP to the kinase induces a conformational change which is transmitted to other areas of the macromolecule.

Pyridoxaloxime, a competitive inhibitor of pyridoxal, was used as a probe of the pyridoxal binding site. It binds to the kinase with a K_I = 2μM and displays a fluorescent decay time of 7.8 nanoseconds. Time emission anisotropy measurements yield a rotational correlation time for bound pyridoxaloxime of approximately 2 nanoseconds, which is considerably shorter than the rotational correlation time of the protein (ϕ =38 nanoseconds). The fast rotation of pyridoxaloxime remains unaffected by the binding of ATP.

A rapid and simple method by which pig brain Pyridoxine-5-phosphate oxidase can be purified in high yield is described. m-Carboxyphenyl-pyridoxamine phosphate (CPP_p), an excellent substrate for pyridoxine-5-phosphate

oxidase, was used as a fluorescent probe for the catalytic site. The fluorescence enhancement detected upon mixing the apoenzyme with Cpp_p suggested the interaction of this synthetic substrate and protein. This result indicated that the substrate recognized its binding site even in the absence of the cofactor FMN.

TABLE OF CONTENTS

LIST OF FIGURES

FIGURE PAGE

LIST OF ABBREVIAIONS

I-EDANS: N-iodoacetylaminoethyl-5-naphthylamine-1-sulfonic acid

TNP-ATP: 2'(3')-trinitrophenyladenosine-5'-triphosphate

PNP: pyridoxine-5-phosphate

PLP: pyridoxal-5-phosphate

CPP_p: m-carboxyphenyl-pyridoxamine phosphate

NPA: p-nitrophenyl anthranilate

FMN: flavin mononucleotide

GOD: glucose oxidase

EDTA: (ethylenedinitrilo)-tetraacetic acid

CHAPTER I

BRAIN PYRIDOXAL KINASE

I. Introduction

The formation of pyridoxal-5-P from ATP and a divalent cation (Zn^{++}) is catalyzed by pyridoxal kinase, an enzyme which has been detected in several mamalian tissues (1). Procedures for the purification of pyridoxal kinase from bovine and porcine brains have been developed in two laboratories (2,3). More recently, it was shown that the mechanism by which brain slices concentrated extracellular vitamin B_6 is related to the enzymatic activity of pyridoxal kinase (4). Despite these studies which suggested the role played by pyridoxal kinase in the transport and metabolism of vitamin B_6, little is known about the mechanism of action of pyridoxal kinase. The aim of the present investigation is 2-fold. Firstly, to study the mechanism of action of pyridoxal kinase by using steady state kinetic methods and secondly, to investigate the effect of ATP binding on the conformation of the enzyme. Two different experimental approaches were used in the binding studies.

One approach consisted of monitoring the interaction of ATP with intrinsic chromophores covalently bound to the protein. The second approach consisted of using pyridoxaloxime as a fluorescent probe for the pyridoxal

binding site. The fluorescence properties, i.e., decay time and emission anisotropy, of bound pyridoxaloxime were monitored by nanosecond spectroscopy.

II. Mechanism of Substrate Addition

Materials

Fresh pig brain was acquired from East Tennessee packing company, Knoxville, Tennessee. CM-Sephadex C-50, Sephadex G-100, DEAE-Sephadex A-25 and Sepharose AH were purchased from Pharmacia Fine Chemicals. Pyridoxal, glutathione and ATP from Sigma. 2'(3')-trinitrophenyl-adenosine-5'-triphosphate (TNP-ATP) from Molecular Probes, Inc. 4-Deoxypyridoxyl-Sepharose was prepared by the method of Kwok and Churchich (3). Hydroxylapatite was prepared by the method of Tiselius (5).

Methods

Purification of the kinase. Pyridoxal kinase from pig brain was purified by procedure developed in our laboratory (6). Pig brains were placed in ice as quickly as possible after slaughter, and preparation began within 1 hour. All enzyme preparation procedures were carried out at $4^{o}C$.

Enzymatic assay. The rate of formation of pyridoxal-5-P was measured by following the increase in absorbance at 388 nm at which pyridoxal-5-P is known to have a molar

extinction coefficient of 4,900 $M^{-1}cm^{-1}$ at pH 7.

The enzymatic activity of pyridoxal kinase was measured at pH 6 in 0.075M potassium phosphate containing pyridoxal (0.1mM), ATP (0.1mM) and $ZnCl_2$ (0.1mM). A molecular weight of 60,000 for pyridoxal kinase with a specific activity of 70 units/mg at pH 6 was used in the calculations of molar enzyme concentrations. A unit of specific activity is defined as the amount of protein which catalyzes the formation of 1 nmol of pyridoxal-5-P/min at 25°C.

Initial rate measurements were carried out by monitoring the change in absorbance at 388 nm for at least 3 minutes in a double beam spectrophotometer (aminco DW 2) set at 0.1 absorbance full scale. The initial velocity data were fitted by a least squares method to the Lineweaver-Burk Transformation of Equation 1a..

$$v = V\,[S]/(K + [S]) \qquad (1a)$$

where S represents the concentration of the varied substrate and K the Michaelis constant. These results agree quite acceptably with the Eadie-Hofstee plots when the linear form (Equation 1b)

$$v = -Kv/S + V \qquad (1b)$$

was used. A modified computer program based on a simple least squares treatment of these alternative linear forms of Michaelis-Menton equation was used to analyze the inhibition patterns (27).

Results

Double reciprocal plots of initial velocity versus pyridoxal of ATP concentrations gave rise to an intersecting pattern of straight lines which are consistent either with a sequential ordered or a rapid equilibrium random mechanism for the addition of substrates (2,3). Several pyridoxal and ATP analogues have reversible competitive inhibitory effect by competing with pyridoxal, whereas TNP-ATP binds to the nucleotide site of the protein (Table 1). The competitive inhibitors of substrate could be used to differentiate between random and ordered mechanism. This protocol is quite likely the simplest approach for making a choice of mechanism between Ordered and Random Bi-Bi possibilities. The rapid equlibrium random pathway of enzyme and subtrate interaction (Random Bi-Bi) is illustrate in Scheme I.

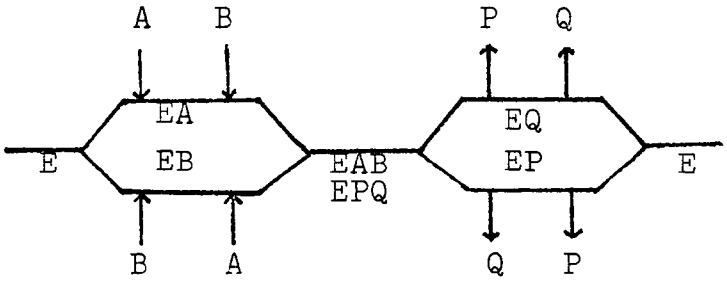

(Scheme I)

In the case of competitive inhibitor for substrate A, the inhibitor, I, would participate in every step in the kinetic mechanism in which the substrate normally reacts. Thus the following interactions of enzyme with inhibitor I may be expected:

$$E + I = EI,\ K_i;\ EB + I = EBI,\ K_{ii};\ EI + B = EIB,\ K_{iii} \quad (2)$$

When the expressions EI and EIB are added to the conservation of enzyme term, and the rate equation derived for the effect of competitive inhibitor of substrate A, the following initial rate relationship is obtained.

$$\frac{1}{v} = \frac{1}{V_1} + \frac{K_a}{V_1(A)}\left[1 + \frac{I}{K_{ii}}\right] + \frac{K_b}{V_1(B)} + \frac{K_{ia}K_b}{V_1(A)(B)}\left[1 + \frac{I}{K_i}\right] \quad (3)$$

When double reciprocal plots of 1/v as a function of 1/A are made at different fixed concentrations of inhibitor, only the slope term of the rate expression is altered; i.e.,

$$\text{slope} = \frac{K_a}{V_1}\left[1 + \frac{I}{K_{ii}}\right] + \frac{K_{ia}K_b}{V_1(B)}\left[1 + \frac{I}{K_i}\right] \quad (4)$$

On the other hand, when B is the variable substrate, double reciprocal plots at different fixed levels of inhibitor will exhibit increases in both slopes and intercepts.

$$\text{Intercept} = \frac{1}{V_1}\left[1 + \frac{K_a}{A}\left(1 + \frac{I}{K_{ii}}\right)\right] \quad (5)$$

$$\text{Slope} = \frac{1}{V_1}\left[K_b + \frac{K_{ia}K_b}{A}\left(1 + \frac{I}{K_i}\right)\right] \quad (6)$$

Equation 3 predicts then that a dead end competitive inhibitor for substrate A of the Random Bi-Bi mechanism is a noncompetitive inhibitor of substrate B.

If now a dead end competitive inhibitor for substrate B is used, the following interactions are to be expected:

$$E + I = EI,\ K_i;\ EA + I = EAI,\ K_{ii};\ EI + A = EIA,\ K_{iii} \quad (7)$$

The rate equation for the effect of a dead end competitive inhibitor of substrate B is described by Eq. 8.

$$\frac{1}{v} = \frac{1}{V_1} + \frac{K_a}{V_1(A)} + \frac{K_b}{V_1(B)}\left[1 + \frac{I}{K_{ii}}\right] + \frac{K_{ia}K_b}{V_1(A)(B)}\left[1 + \frac{I}{K_i}\right] \quad (8)$$

It is clear from Eq. 8 that a dead end competitive inhibitor of substrate B will show noncompetitive inhibition relative to substrate A. In summary then, for the random Bi-Bi mechanism, a competitive inhibitor for either substrate will act as a noncompetitive inhibitor for the other substrate. These observations are consistent with the symmetry inherent in the random mechanism.

The inhibition kinetic patterns of TNP-ATP are included in Figures 1 and 2. It can be seen that TNP-ATP is a competitive inhibitor with respect to ATP, whereas it acts as a noncompetitive inhibitor with respect to pyridoxal when the concentration of ATP is kept constant. These inhibition kinetic patterns, included in Table 1, are consistent with a random mechanism for the addition of substrates.

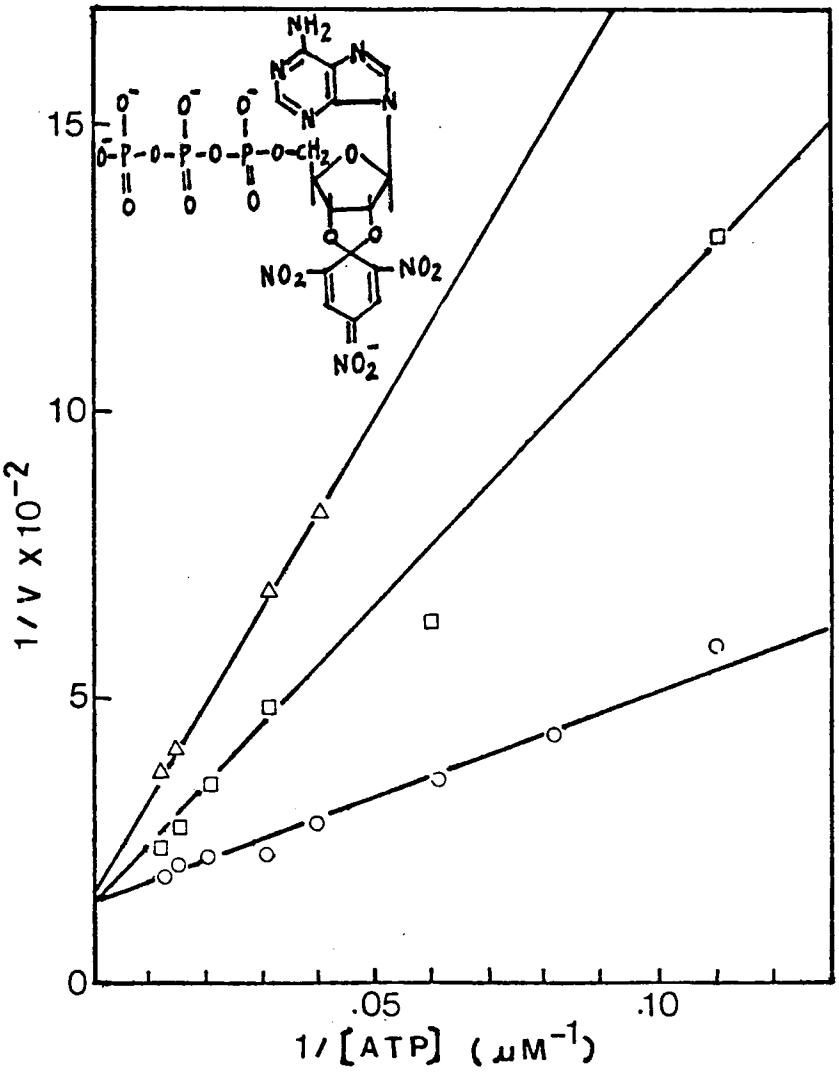

Figure 1. Kinetics of inhibition of pyridoxal kinase by TNP-ATP. Lineweaver-Burk plots of initial rates of the forward reaction versus ATP concentrations in the presence of 0(○), 1.2(□), and 1.7μM(△) TNP-ATP. The concentration of pyridoxal (0.1mM) was held constant in 0.075M potassium phosphate (pH 6)containing 0.1 mM $ZnCl_2$. Velocity is expressed as change in absorbance at 388 nm per minute.

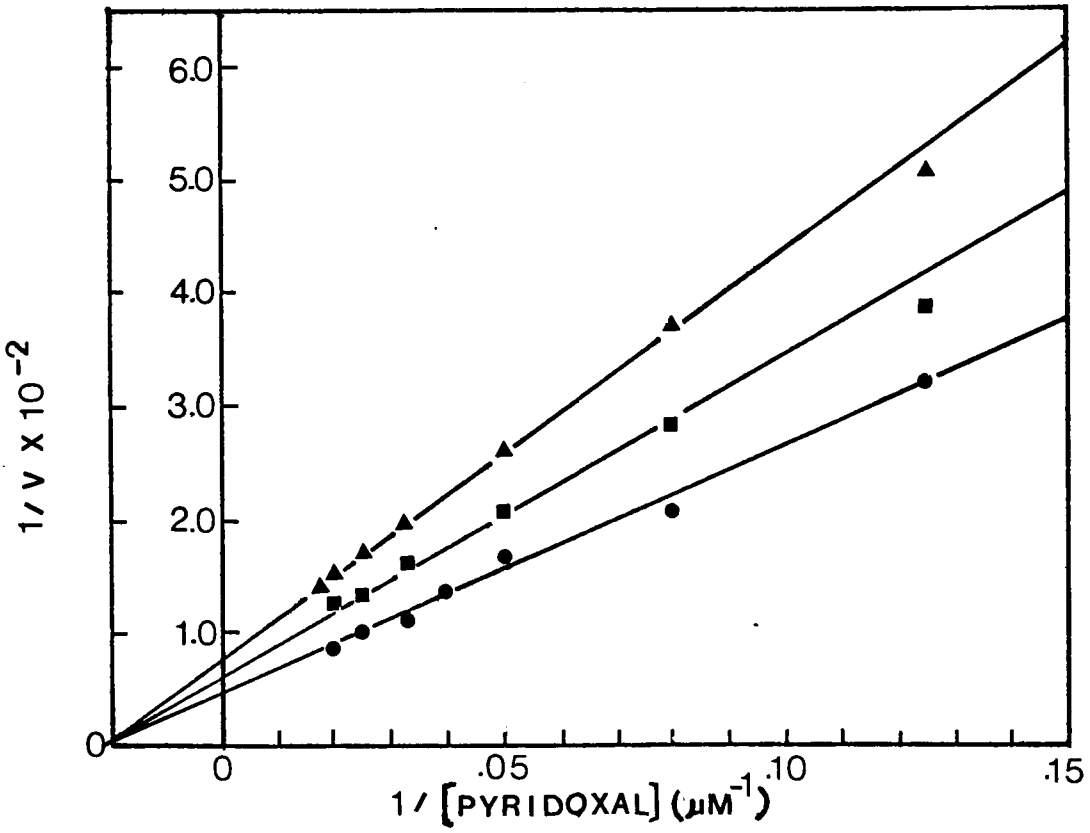

Figure 2. Lineweaver-Burk plots of initial rates of the forward reaction versus pyridoxal concentrations in the presence of 0(●), 0.53(■) and 0.74μM(▲) TNP-ATP. The concentration of ATP(0.1mM) was held constant in 0.075M potassium phosphate(pH 6) containing 0.1mM $ZnCl_2$. Velocity is expressed as change in absorbance at 388 nm per minute.

Table 1. Inhibition of Pyridoxal Kinase by Compounds Structurally Related to Pyridoxal and ATP

Inhibitor	Varied Substrate	Pattern	K_I
TNP-ATP	ATP	Competitive	5.1×10^{-7}M
	Pyridoxal	Noncompetitive	8×10^{-7}M
Pyridoxaloxime	ATP	Noncompetitive	1.5×10^{-6}M
	Pyridoxal	Competitive	2×10^{-6}M

III. Binding of ATP

Materials

N-iodoacetylaminoethyl-5-naphthylamine-1-sulfonic acid (1-5-I-EDANS) was purchased from Molecular Probes, Inc. ATP was obtained from Sigma.

Methods

Binding of ATP. Indirect binding studies utilized titrations of intrinsic protein fluorescence to determine binding parameters. Fluorescence measurements were performed using a fluorimeter equipped with two Bausch and Lomb monochromators. Excitation and emission wavelengths were 290 and 340 nm, respectively.

Labeling of the enzyme. Pyridoxal kinase at a concentration of 2 mg/ml was allowed to react with 1 mM 1-5-I-EDANS at pH 6.8. The reaction was allowed to proceed for 5 h at 4°C. The excess reactant was removed by gel filtration through Sephadex G-25, equilibrated with 0.075M potassium phosphate (pH 6). The degree of labeling of the protein was determined spectrophotometrically using an extinction coefficient of $6.2 \times 10^3 M^{-1} cm^{-1}$ at 340 nm. The labeled enzyme was fully active and contained 1 mol of 1-5-I-EDANS/mol of enzyme.

Results

The emission spectra recorded in Fig. 3 shows that

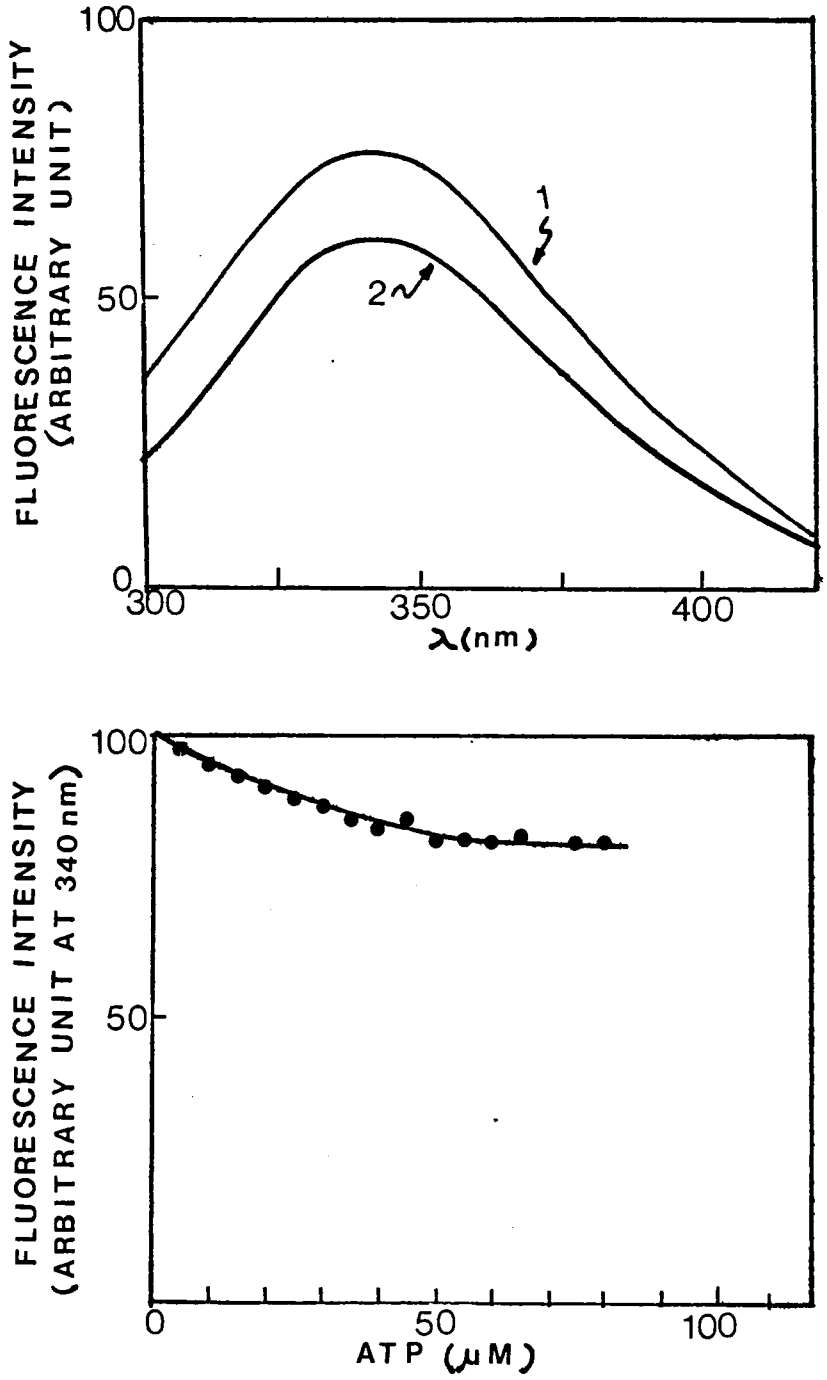

Figure 3. (Upper) Emission spectra of pyridoxal kinase(10μM) in the absence(1) and presence(2) of ATP(50μM) in 0.075M potassium phosphate(pH 6) containing $ZnCl_2$(0.1mM). Excitation wavelength 295 nm. (Bottom) Change in the fluorescence intensity at 340 nm upon addition of increasing concentrations of ATP to a solution of the enzyme(10μM) in 0.075M potassium phosphate(pH 6) containing $ZnCl_2$(0.1mM).

the binding of ATP to the kinase induces quenching of protein fluorescence. The quenching effect associated with protein-ATP complex formation was used to determine the affinity of ATP for the nucleotide site of the enzyme. In these experiments, fluorescence intensities of samples containing a fixed concentration of protein and varying concentrations of ATP were measured after a 15 minutes incubation at 25°C. Figure 3 shows the change in protein fluorescence upon the addition of increasing concentrations of ATP. At ATP concentration of 50 μM, the relative fluorescence intensity (F/F_o) approaches the limiting value of 80%. The fraction of binding sites (θ) occupied by ATP was determined by Equation 9.

$$\theta = \frac{F_o - F}{F_o - F_m} = \frac{[E - ATP]}{[E_t]} \qquad (9)$$

where F is the fluorescence observed when free and complexed enzymes are in equilibrium, F_o is the fluorescence intensity of the enzyme in the absence of ATP, and F_m the fluorescence observed at an ATP concentration of 50 μM. Application of the law of mass action for one binding site per molecule of enzyme gives the following relationship between the fraction of binding sites occupied (θ) and the concentration of free ATP (Equation 10).

$$1 / (1 - \theta) = K_A [ATP] \qquad (10)$$

A plot of $\theta/1-\theta$ versus [ATP] yields an association

constant (K_A) of 4 x $10^4 M^{-1}$ for the binding of one molecule of ATP per molecule of enzyme. The dissociation constant determined by fluorometric titrations compares well with the K_M of the kinase for ATP (20μM) as determined by enzymatic methods (3).

The quenching of protein fluorescence elicited by the binding of ATP can be attributed either to conformational changes of the enzyme or to a direct interaction between the adenine moiety of ATP and vicinal aromatic amino acid residues of the protein. In an effort to obtain information about indirect effects of ATP binding on protein conformation, the interaction of ATP with the enzyme labeled with an extrinsic chromophore was examined by means of fluorescence spectroscopy.

Previous studies in our laboratory have shown that cysteinyl amino acid residues of pyridoxal kinase are not involved in the binding of the substrates ATP and pyridoxal. Thus, the reaction of one SH group per molecule of enzyme with the fluorescent chromophore I-EDANS has no effect on the catalytic properties of the kinase (8).

The binding of ATP to the kinase tagged with I-EDANS brings about a decrease in the fluorescence emitted by the extrinsic chromophore upon excitation with light of 360 nm. As shown in Fig. 4, the extent of fluorescence quenching depends on the degree of occupation of the binding site by ATP and reaches a maximum at 25% of the total fluorescence

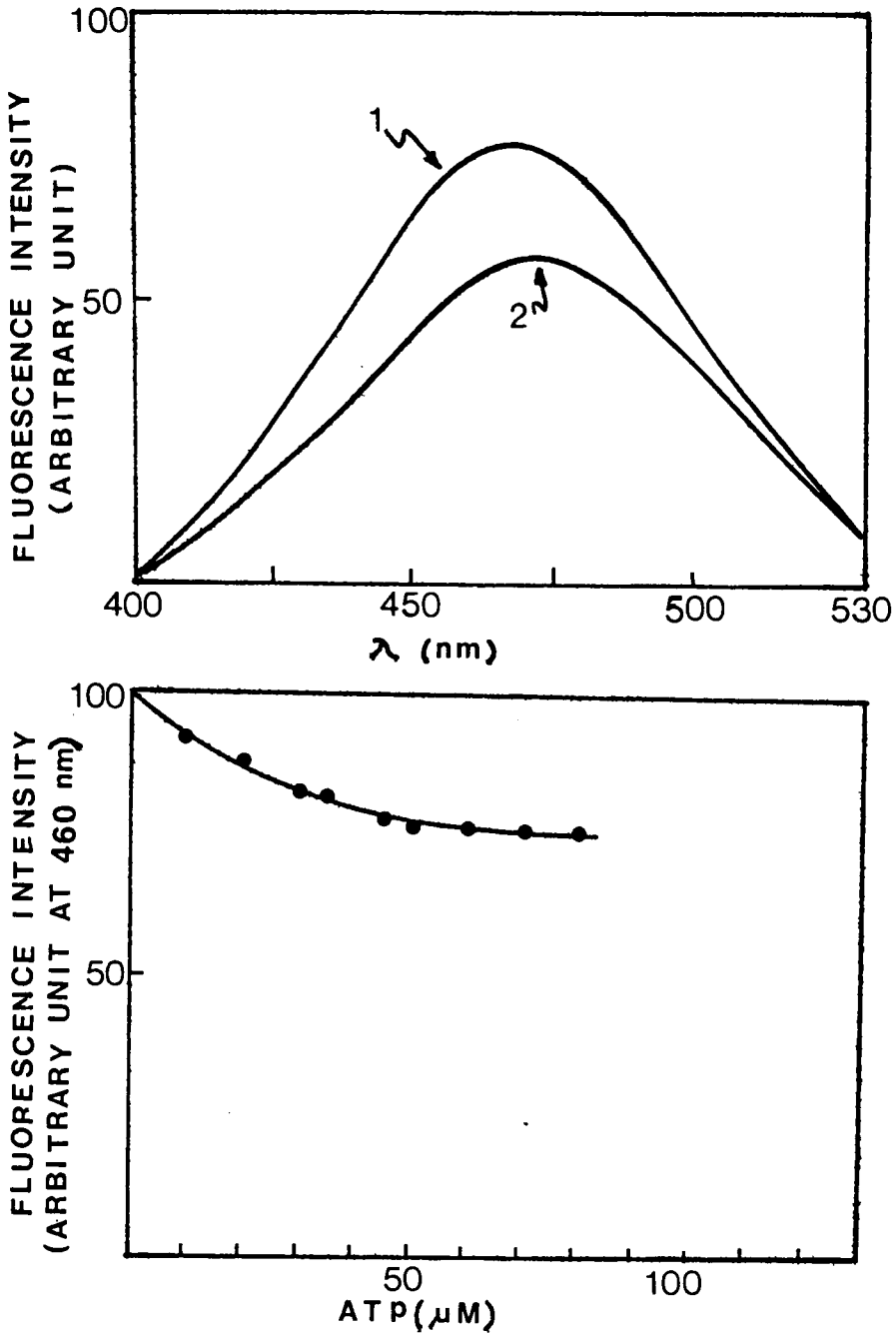

Figure 4. (Upper) Emission spectra of I-EDANS-kinase (10uM) in the absence(1) and presence(2) of ATP (50uM) in 0.075M potassium phosphate(pH 6) containing $ZnCl_2$(0.1mM). Excitation wavelength 360 nm. (Bottom) Change in the fluorescence intensity at 460 nm upon addition of increasing concentration of ATP to solution of I-EDANS-kinase(10uM).

when the concentration of ATP is 50 μM. Further increase in ATP to a final concentration of 90 μM has no effect on the extent of fluorescence quenching (Fig. 4). Since the fluorescent chromophore is covalently bound to a site on the enzyme distinct from the nucleotide site, it seems reasonable to suggest that conformational perturbations caused by the binding of ATP to the nucleotide site are transmitted to other areas of the protein macromolecule.

IV. Binding of Pyridoxaloxime

Materials

ATP was purchased from Sigma. 1-5-I-EDANS was from Molecular Probs, Inc. Pyridoxaloxime was synthesized and donated by Dr. Francis Kwok.

Methods

The procedures for the labeling of the enzyme with 1-5-I-EDANS was the same as described in methods of section III.

Spectroscopy. Fluorescence spectra were recorded in a precision spectrofluorimeter equipped with two Bausch and Lomb monochromators. The slits of the monochromators were set to give a band width of 3 nm. Polarization fluorescence measurements were conducted in an instrument described by Churchich(9). Illumination was provided by a Xenon lamp (150 watts) with wavelengths selected by a

quartz prism monochromator. The band width for excitation was 5 nm. Fluorescence polarized light emitted by the labeled enzyme sample passed through Corning glass filters.

Fluorescence decay measurements were made using the monophotonic technique with an Ortec model 8200 nanosecond spectrometer. Time base calibration of the multichannel analyzer was performed indirectly using a solution of quinine sulfate in 0.1N sulfuric acid.

A free runing flash lamp operating in air at 1 ATM was used as the exciting source. The lamp was pulsed at 10 KHZ. Excitation was set at 340 nm and the emission was filtered through a Corning glass filter (C-5-3-72). Rotational relaxation times were determined by recording the fluorescence decay curves of the polarized components $F_{\parallel}(t)$ and $F_{\perp}(t)$, parallel and perpendicular, respectively, to the plane of the incident polarized light. Polaroid HNB sheet polarizers were used for excitation and emission. The functions $D(t) = F_{\parallel}(t) - F_{\perp}(t)$ and $S(t) = F_{\parallel}(t) + 2F_{\perp}(t)$ were deconvoluted and the deconvoluted decay functions were each accurately fitted to monoexponential decay using nonlinear least squares analysis.

For a chromophore rotating in common with a rigid sphere, the emission anisotropy function $A(t) = D(t)/S(t)$ decays in a monoexponential manner (Eq. 11)

$$A(t) = A_o e^{-t/\phi} \qquad (11)$$

and the rotational correlation time (ϕ) is obtained by plotting Log A(t) versus time. Equation 11 was used in the determination of the rotational correlation time of I-EDANS-kinase.

Evaluation of fluorescence lifetimes. Ideally, in order to determine fluorescence lifetimes, a lamp pulse of extremely short duration, relative to the fluorescence lifetime, should be used to excite the sample solution, and the solution emission monitored and recorded by a very fast response detector system. the fluorescence lifetime can then be easily evaluated from the solpe of semilog plot of emission intensity versus time. In reality, for many systems, the lamp pulse duration may be of the same order of magnitude as the fluorescence lifetime. In addition, the detector system may produce signal distortion. Evaluation of lifetimes under these conditions is not as straightforward as in the ideal case. It was desired to empoly a procedure which was precise and accurate and which provided reasonable direct and objective evaluation of lifetimes. The Demas-Adamson evaluation is straightforward (10), requiring only that the lamp intensity decay data and sample fluorescence decay data be known in arbitrary intensity scale units relative to a common time scale. Furthermore, in contrast to some methods, the lamp decay maximum intensity need not be normalized to the sample intensity, a factor which facilitates data reduction. The

decay data for lamp and sample are transformed into new functions of time:

$$W(t) = \frac{EX(t)}{\int_0^t EX(t)\,dt} \qquad (12)$$

$$Z(t) = \frac{\int_0^t EM(t)\,dt}{\int_0^t EX(t)\,dt} \qquad (13)$$

These two functions, W(t) and Z(t), are then related by Equation 14.

$$Z(t) = -\tau_F W(t) + K\tau_F \qquad (14)$$

where τ_F is the desired fluorescence lifetime and K is a constant which has no interpretive significance (its value will depend on the relative intensities of EM and EX). A plot of Z(t) versus W(t) will have a slope of $-\tau_F$. There will be as many (W,Z) data pairs as there are EM and EX data points. This number is chosen rather arbitrarily, but the choice is made with the consideration that more data per unit time will yield better precision through a better trapezoidal approximation while increasing the time required for clerical aspects of data reduction. The computer program described in Appendix A was used to deconvolute the data based on the least square method developed by Demas (10). The program written was adapted from that of Dr. Georghiou in the Dept. of Physics.

Results

Pyridoxaloxime was chosen as a probe of the pyridoxal binding site for the following reasons: a) it exerts an inhibitory effect on kinase activity by competing with pyridoxal. The inhibition constant for pyridoxaloxime is 2μM, whereas the dissociation constant for pyridoxal is 11μM (3); b) the binding of pyridoxaloxime to the protein, due to the high fluorescence quantum yield of the inhibitor (q = 0.21) can be easily monitored by steady emission anisotropy. At a protein concentration of 50μM and pyridoxaloxime concentration of 10μM, the binding of the inhibitor results in an increase in emission anisotropy from 0.02 to 0.1 (Table 2); and c) upon excitation with nanosecond pulses, the emission of pyridoxaloxime decays with a fluorescent lifetime of 7.8 nanoseconds (Fig.5), which can be used conveniently to determine the rotational correlation time of the bound inhibitor.

Time dependent emission anisotropy measurements were performed at a protein concentration of 50μM and pyridoxaloxime concentration of 10μM to ensure binding of the inhibitor to the enzyme. Under these experimental conditions, the protein concentration is 25 fold greater than the dissociation constant (K_D = 2μM) of the inhibitor and the fraction of ligand bound approaches 1, i.e., all the inhibitor in solution is stoichiometrically bound. The results of the time dependent emission anisotropy

Table 2. Fluorescence Properties of I-EDANS-Kinase and Pyridoxaloxime Bound to the Kinase

	Fluorescence Maximum (nm)	Fluorescence Decay Time (n.s.)	Emission Anisotropy	Rotational Correlation Time (n.s.)
I-EDANS-Kinase (10uM)	470	19.1	0.24	38
Pyridoxaloxime (10uM)	455	7.8	0.02	--
Pyridoxaloxime (10uM) + Enzyme (50uM)	455	7.8	0.10	2

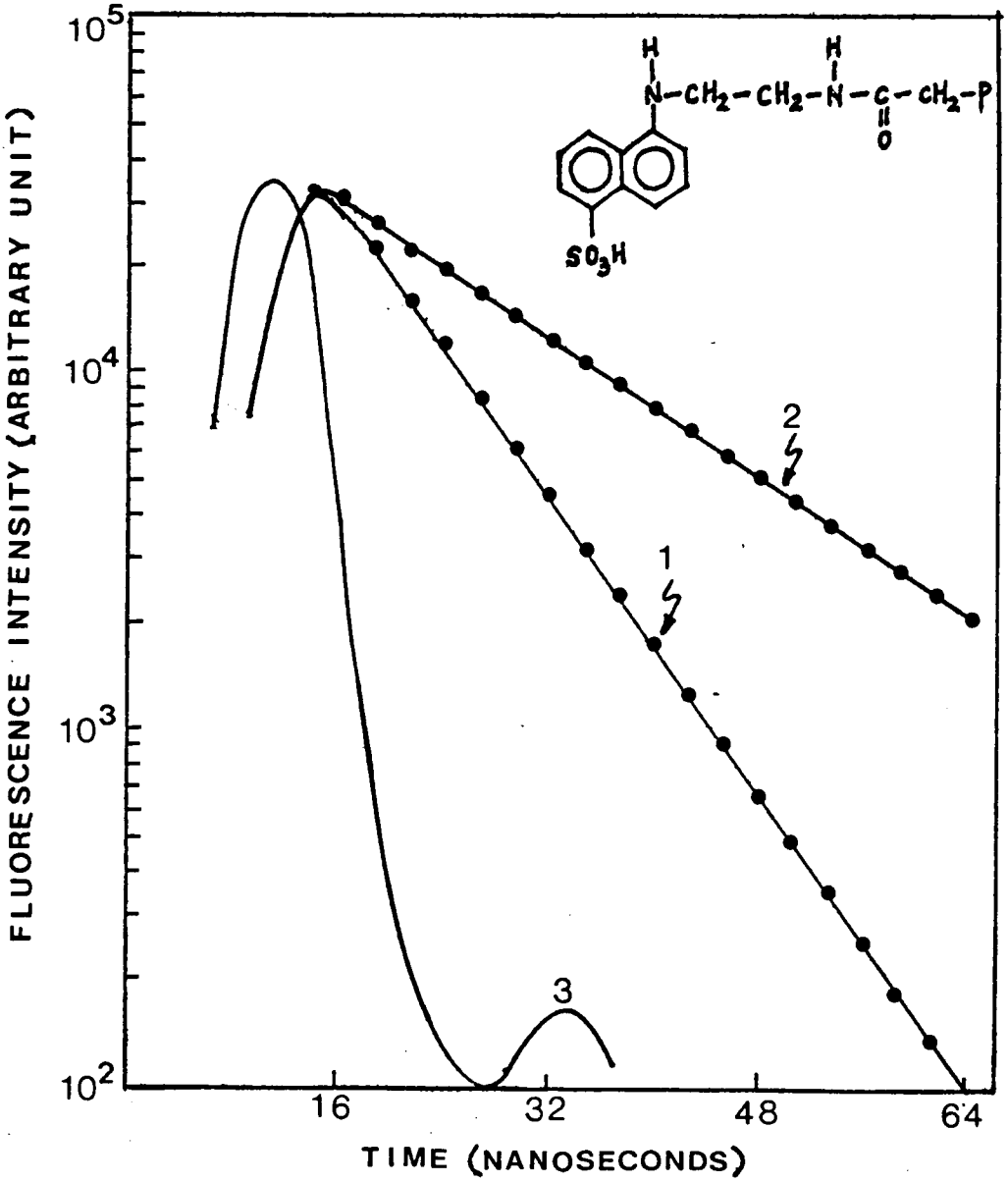

Figure 5. Fluorescence decay kinetics of I-EDANS-kinase(2) and pyridoxaloxime + kinase(1) in 0.075M potassium phosphate(pH 6) obtained with the monophotonic fluorescence technique. The lamp profile(3) is included in the figure.

measurements indicate that a very fast initial decay of the emission anisotropy function took place in less than 6 nanoseconds (Fig. 6). The absence of any long rotational correlation time component in the observed anisotropy kinetics comparable in magnitude to the calculated rotational correlation time of the macromolecule (ϕ = 35 n.s.) strongly suggests that the bound inhibitor displays a very high degree of rotational mobility.

It is interesting to note that ATP at a final concentration of 0.1mM has no effect on the observed emission anisotropy decay of bound pyridoxaloxime (Fig. 6).

In marked contrast to pyridoxaloxime, the fluorescent probe I-EDANS covalently bound to a SH group appears to be immobilized by strong interactions with the protein matrix. A representative set of experimental data for the emission anisotropy decay of the dansylated enzyme is given in Fig. 6. It is immediately apparent from the observed anisotropy kinetics that a long rotational correlation component (ϕ = 38 n.s.) could be unambiguously assigned to the rotation of the entire macromolecule.

V. Discussion

The inhibition kinetic patterns obtained when ATP and pyridoxal analogues are used as dead-end inhibitors of the reaction catalyzed by the kinase are consistent with a rapid equilibrium random Bi-Bi, in which binary complexes,

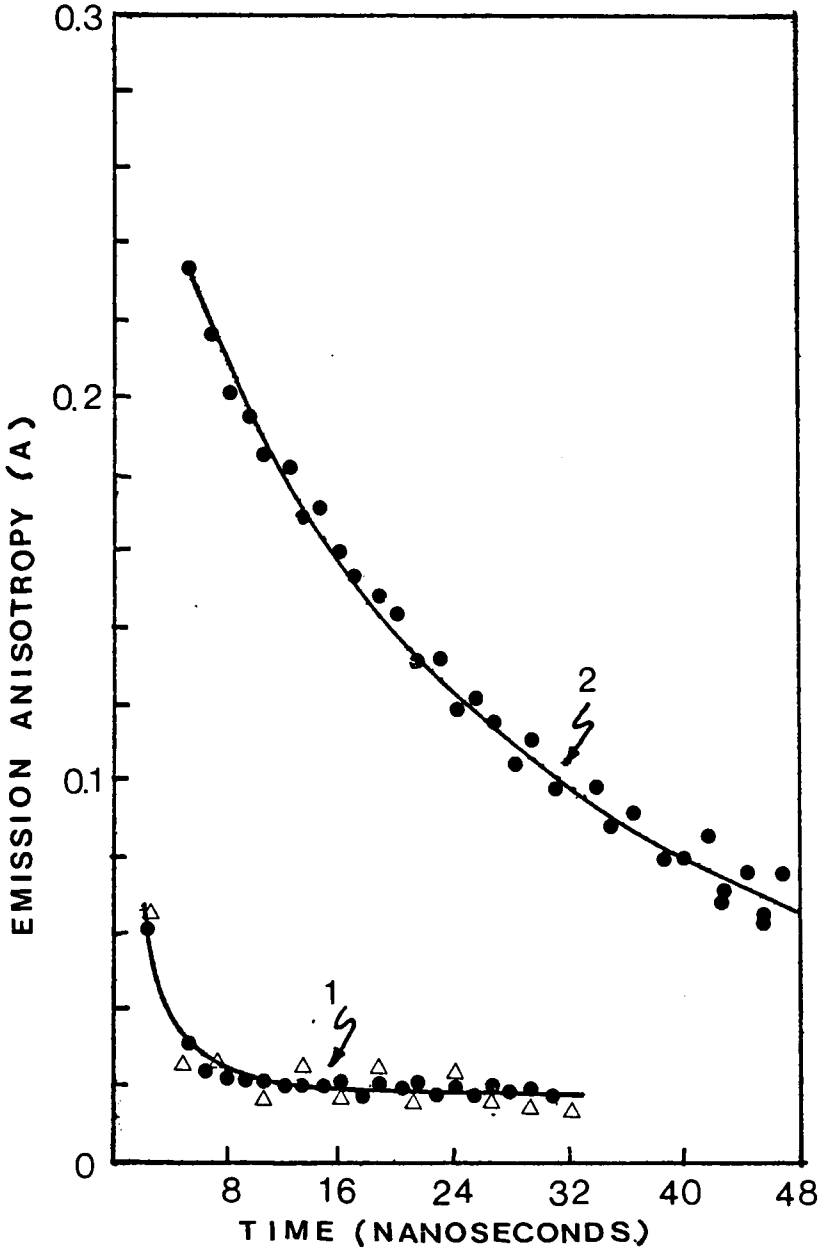

Figure 6. Comparision of the emission anisotropy kinetics of I-EDANS-kinase(50uM) (curve 2) and the mixture kinase + pyridoxaloxime(10uM) (curve 1) in the absence(●) and presence(△) of ATP(1mM) at pH 6. The best fit parameters for I-EDANS-kinase are τ =19.1 nanoseconds, A_o = 0.24 and ϕ =38 nanoseconds. The best fit parameters for the fast initial decay of the emission anisotropy function of bound pyridoxaloxime are τ = 7.8 nanoseconds, A_o = 0.30 and ϕ = 2 nanoseconds.

i.e.,enzyme-ATP and enzyme-pyridoxal, are formed in kinetically significant amounts. Based on these kinetic observations, the reaction catalyzed by pyridoxal kinase can be represented by the following scheme:

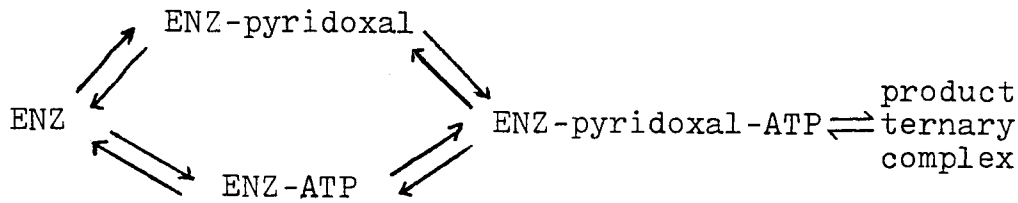

The formation of binary complexes in solution was also demonstrated by independent binding studies designed to determine the dissociation constants of ATP and pyridoxal. In the present work, protein fluorescence quenching was used to determine the dissociation constant of the binary complex enzyme-pyridoxal (3). An important result of the binding studies is the finding that the dissociation constants obtained for ATP and pyridoxal, K_D = 25μM and K_D = 11μM, respectively, agree within experimental error with the K_M values derived from enzymatic measurements (3). The binding of ATP to the kinase induces changes in protein fluorescence that can be attributed either to conformational changes of the protein or to direct interaction between the adenine moiety of ATP and vicinal tryptophyl residues.

Fluorescence quenching due to a dipole-dipole coupling process depends on the reciprocal of the sixth power of the distance R between chromophores, and on the

critical Forster's transfer distance R_o at which the efficiency of transfer is 50% (11). Due to the small value of the overlap integral ($J = 1.4 \times 10^{-9} cm^3 M^{-1}$) of the absorption spectrum of ATP and trytophan emission of the protein, the critical distance of transfer for the tryptophan-ATP pair is only 5Å. Hence, the presence of one or more trytophan residues at the nucleotide site might induce significant effects on protein fluoresence upon addition of ATP.

It follows from these considerations that measurements of protein fluorescence alone cannot be taken as evidence of conformational changes of the macromolcule. Information about indirect effects of binding on protein conformation was obtained from fluorescence measurements of a chromophore covalently bound to a cysteinyl residue which was not positioned at the nucleotide site of the enzyme. The results of those spectroscopic measurements showed that very low concentrations of ATP (50μM) was needed to influence the band position as well as the fluorescence quantum yield of the extrinsic chromophore tagged to the enzyme. These observations are interpreted to mean that perturbations caused by the binding of ATP are transmitted to other areas of the protein. It is worthy of note that these conformational fluctuations do not influence the rapid rotation of pyridoxaloxime bound to the pyridoxal site. The rotational correlation time

observed for pyridoxaloxime bound to kinase is abnormally short, and it is worth inquiring as to its origin. The simplest explanation is that the short rotational correlation time value is due to a high degree of rotational mobility of the inhibitor bound to the pyridoxal binding site. Supporting this view are the steady emission anisotropy measurements of pyridoxaloxime complexed to the enzyme. Thus the emission anisotropy of bound pyridoxaloxime (A = 0.10) is low when compared to the emission anisotropy of pyridoxaloxime immersed in a viscous solvent (A = 0.31). This difference in emission anisotropy values reflects the rotation of the fluorescent inhibitor during the decay time of 7.8 nanoseconds.

Alternatively, there is the possibility that pyridoxaloxime bound to a protein site distinct from the pyridoxal binding site is relatively insensitive to the conformational changes induced by ATP. While this explanation seems attractive, it may be disputed on the basis that pyridoxaloxime is a competitive inhibitor with respect to pyridoxal. In addition, the steady emission anisotropy measurements of pyridoxal bound to the catalytic site have revealed that the substrate is not immobilized by the protein matrix (3).

In view of these considerations, it seems reasonable to propose that the short correlation time of bound pyridoxaloxime is primarily the result of a weak strain

induced by amino acid residues located at the catalytic site. If the same concept is appropriate for the binding of the substrate pyridoxal, then a nonproductive conformation of the enzyme-substrate complex would decrease the enzyme's catalytic power. Perhaps, this is the main reason for the low specific activity of pyridoxal kinase.

CHAPTER II

BRAIN PYRIDOXINE-5-PHOSPHATE OXIDASE

I. Introduction

Recently, pig brain pyridoxine-5-P oxidase (EC 1.4.3.5) was purified to electrophoretic homogeneity in our laboratory (8). Here, a rapid and simple method by which the enzyme can be purified in high yield is described. An easily prepared affinity chromatography support, phosphopyridoxyl Sepharose, was employed in the purification. This method allowed total purification of pyridoxine-5-P oxidase from the same tissue source in five days. The enzyme preparation migrated as three protein bands and three activity bands on analytical gel electrophoresis.

Pyridoxine-5-P oxidase is an FMN-dependent enzyme involved in the conversion of vitamin B_6 to pyridoxal-5-P and may be important in regulating B_6 metabolism (12). This enzyme is made up of two subunits of 30,000 molecular weight (8). It catalyzes O_2 dependent oxidation of not only the 4-aminomethyl and 4-hydroxymethyl substituent of the phosphorylated vitamers but also secondary amines at the 4' position (13). To further understand the nature of the active site of this flavoprotein, the fluorescence spectra of enzyme-substrate was examined. m-Carboxyphenyl-pyridoxamine phosphate (CPP_p), which is a substrate for

PNP oxidase with K_M = 1μM, was found to be a good fluorescence probe in the study of the catalytic site of enzyme. Studies of binding of CPP_p to apoPNP oxidase showed a fluorescence enhancement for CPP_p. These results implies the interaction between enzyme and substrate either in the presence or absence of cofactor FMN.

II. Rapid Purification of PNP Oxidase

Materials

Pyridoxal-5-P, nitroblue-tetrazolium, glutatione and sodium borohydride were purchased from Sigma Chemical Company. Pyridoxine-5-P was prepared by reduction of PLP by sodium borohydride. Potassium phosphate (monobasic and dibasic) and ammonium sulfate were from Fisher. Sephadex G-100, CM-Sephadex C-50, Sepharose 4B and AH-Sepharose were purchased from Pharmacia Fine Chemicals.

Methods

Preparation of phosphopyridoxal Sepharose. The methods employed was adapted from that of Cash et al. (15). Six grams of commercially available ω-aminohexyl Sepharose was suspended in 50 ml of water, brought to pH 7 by addition of 1N NaoH, and mixed with 1 gm of pyridoxal-5-P. The slurry was gently shaken for 12 hr in the dark at room temperature. The resulting Schiff base was reduced by addition of 20 mg of solid sodium borohydride at 4°C.

After all traces of yellow color had disappeared, the slurry was allowed to reach room temperature and the pH was adjusted to 6 with 7% acetic acid to destroy residual sodium borohydride. When evolution of hydrogen gas had ceased, the slurry was washed several times with water. Then the gel was packed into a 1.6 x 20 cm chromatography column. The column was extensively rinsed with 1M KCl, then with water before use.

Enzymatic assays. For precise kinetic data, the rate of formation of pyridoxal-5-P was measured by following the increase in absorbance at 388 nm at which pyridoxal-5-P is known to have a molar extinction coefficient of 4,900 $M^{-1}cm^{-1}$ at pH 7. Pyridoxine-5-P was used as the substrate for enzymatic assay throughout the whole purification process. The enzymatic assay mixture contained 0.1mM pyridoxine-5-P in 0.1M potassium phosphate (pH 8) in a total volume of 1 ml. One unit of enzymatic activity catalyzes the formation of 1nmol of PLP per minute.

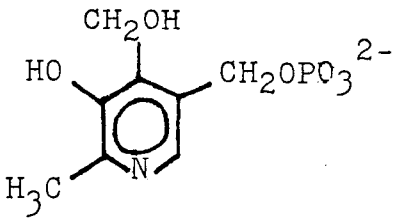

(PNP)

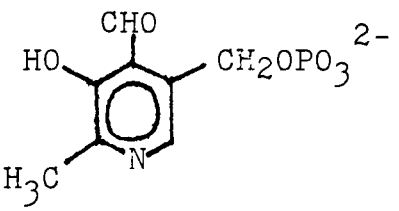

(PLP)

The enzymatic assay of the crude homogenate of pig brain was performed by utilizing the reaction between

pyridoxal-5-P and phenylhydrazine. The product of the reaction gave an absorption maximum at 410 nm (ε_{410nm} = 23,000). This method was used because direct spectrophotometric assay method was hindered by the light scattering effect of the turbid assay solution. The assay mixture was incubated at 25°C for 30 min. After the incubation, 0.1 ml of 100% tricholroacetic acid was added to the assay mixture which was then subjected to centrifugation at 6000 rpm in a desk-top centrifuge for 10 min (DYNAC centrifuge). One ml of the supernatant was removed to another test tube and 0.1 ml of 2N phenylhydrazine in 10N H_2SO_4 was added. The mixture was read by a spectrophotometer at 410 nm after 3 min.

Enzyme purification. Pig brain were obtained from East Tennessee Packing Company. The brains were placed in ice as quickly as possible after slaughter, and preparation began within 1 hr. Enzyme preparation procedures were carried out generally at 4°C. A Waring Blender was used to prepare a 25% (W/V) homogenate in a solution of 0.075M potassium phosphate (pH 6.8). The homogenate was centrifuged at 10,000 x g for 30 min, and the pellet was discarded. The pH of the crude extract was adjusted to 5.0 by the dropwise addition of 2N acetic acid and the resulting suspension stirred for 10 min. The precipitate was removed by centrifugation for 30 min at 10,000 x g and the supernatant was brought to pH 6.8 with 2N NaoH. A slight

precipitation was removed by centrifugation (10,000 x g). The supernatant was then treated with $(NH_4)_2SO_4$. The precipitate obtained at 40 to 60% saturation was dissolved in 0.01M potassium phosphate (pH 6.8), containing 0.1mM glutathione (buffer 1). It was then dialyzed against buffer 1 and applied to a column (35 x 2.6cm) of CM-Sephadex C-50 equilibrated with the same buffer. The column was eluted with buffer 1, the pyridoxine-5-P oxidase were not retained by CM-Sephadex, whereas red contaminating proteins adsorbed to the gel. The fractions containing pyridoxine-5-P oxidase activity were combined, concentrated by ultrafiltration (Amicon XM-100), and chromatographed on a (100 x 2.6cm) of Sepharose-4B previously equilibrated with buffer 1. The fractions contained oxidase were collected and then applied on a column (20 x 2.6cm) of phosphopyridoxyl Sepharose equilibrated with buffer 1. The affinity column was washed with 100 ml of buffer 1 and then 300 ml of buffer 1 containg 300 mM KCl. Pyridoxine-5-P oxidase was eluted with 100 ml of 5mM PLP in distilled water. The fractions containing pyridoxine-5-P oxidase were combined, dialyzed against buffer 1, concentrated by ultrafiltration, and further purified in a column (100 x 1.6 cm) of Sephadex G-100 equilibrated with buffer 1. The fractions containing pyridoxine-5-P oxidase were concentrated by ultrafiltration and stored at $-12^{\circ}C$. Under these conditions, pyridoxine-5-P oxidase remains

stable for at least 2 months. The homogeneity of the enzyme was determined by polyacryamide gel electrophoresis in a water-cooled Buchler polyanalyst (Buchler Instrument) by the method of Davis (16).

Protein determination. The Folin method (17) was employed using bovine serum albumin as standard.

Activity stain of Pyridoxine-5-P oxidase. Purified pyridoxine-5-P oxidase was examined by polyacrylamide gel electrophoresis at pH 8.4 following the procedures of Davis (16) for 7.5% polyacrylamide gels. After electrophoresis at 4°C, pyridoxine-5-P oxidase activity was detected by the method of Feinstein and Lindahl (13). Activity staining mixture contained 7 ml of 100mM PNP in 100mM potassiun phosphate (pH 8) and 0.5 ml of nitroblue-tetrazolium (1 mg/ml).

Results

Table 3 summarizes the purification of the pyridoxine-5-P oxidase from pig brain. The PNP oxidase had been purified 2500-fold from pig brain and 20% of the totle activity was recovered. Fig. 7 shows the protein and activity stain for purified PNP oxidase. Three protein and three activity bands were detected by analytical electrophoresis gels.

Table 3. Purification of Pyridoxine-5-P Oxidase from Pig Brain

Treatment	Volume (ml)	Protein (mg/ml)	Specific Activity (U/mg)	Total Activity (U)
Homogenate	3,100	10.3	0.04	1277
Acid Precipitation(pH5)	3,000	5.2	0.08	1248
40-60% $(NH_4)_2SO_4$ Fraction	130	25.5	0.30	995
CM-Sephadex Fraction	95	24.6	0.35	818
Sepharose 4B Fraction	108	11.6	0.49	615
PLP-Sepharose Fraction	85	0.17	25.00	362
Sephadex G-100 Fraction	10	0.28	90.00	252

Figure 7. The protein and activity stains for purified PNP oxidase after electrophoresis in 7.5% polyacylamide gel.

III. Emission Properties of m-Carboxyphenyl-Pyridoxamine Phosphate and Its Use in The Study of Binding to PNP Oxidase

Materials

Pyridoxal-5-P was purchased from Sigma. 1,4-Dioxane and ethanol was obtained from Fisher, and DL-gabaculine was from Boehringer. Amberlite CG-50 was purchased from Mallinkrodt Chemical Works. 3-Carboxymethyl-FMN was a kindly donation from Dr. K. B. McCormick. Potassium bromide was obstained from Fisher and EDTA was from Matheson Coleman & Bell Manufacturing Chemists.

Methods

Synthesis of m-carboxyphenyl-pyridoxamine phosphate. CPP_p was kindly synthesized and donated by Mr. D. S. Kim in our laboratory (14). A solution of the dipotassium pyridoxal-5-P (1 mmol) was added in small portion to 1 mmol potassium salt of DL-gabaculine in dry methanol (total volume 15 ml). The solution was treated with 0.02M $NaBH_4$ at $4^{\circ}C$ after the reaction was proceeded at $60^{\circ}C$ for 1 hr. The mixture was filtered, acidified with acetic acid and evaporated. The precipitate was dissolved in water and chromatographed on ion exchange resin, amberlite CG-50 (Column 2 x 50cm), with water as the eluting solvent. Fractions absorbing at 330 nm and 290 nm were collected and freeze dried. The purity of the compound was examined by

thin layer chromatography on silica gel plates using the solvent system butanol-water-acetic acid (2:2:1). The purified compound gave a single spot on thin layer chromatography.

Synthesis of PLPoxime. Two gram of PLP was dissolved in 50 ml of methanolic potassium hydroxide (MeKOH). 0.25 gm of NH_2OH was added and reaction mixture was refluxed for 4 hr. The solution was evaporated and the precipitate was dissolved in water and chromatographed on ion exchange resin, amberite CG-50, with 0.5N HCl as the eluting solvent. The fractions absorbing at 342 nm was collected and concentrated.

Spectroscopy. Fluorescence measurement and evaluation of fluorescence lifetime were the same as described in methods of section III, Chapter I. Instrumentation for phosphoresence investigation was identical to that described for fluorescence measurement with the addition of rotating slotted disk and provision for immersion of the sample in a Dewar for liquid nitrogen temperature ($77^{\circ}K$). Excitation light from a Xenon lamp, after dispersion by the excitation monochromator, is admitted to the sample via a fixed slit system and a set of slotted disks with equally spaced ports rotating around the sample cuvette. The slots were so arranged that openings in one are in line with uncut portions of the second disk. Thus the sample is alternately

exposed to and shielded from the excitation light: while it is dark the phosphorescence was passed to the emission monochromator and hence to the detector system. Decay curve of phosphorescence can be recorded by following the decay in the intensity of phosphorescence with time after the removal of the excitation light. The solvent used was ethanol. When cooled to liquid nitrogen temperature, it formed a clear transparent solid.

Results

It has been previously reported that m-carboxyphenyl-pyridoxamine phosphate has an absorption maximum at 320 nm ($\log \varepsilon = 3.74$) at neutral pH. It fluoresces at 415 nm when excited with light at 317 nm (19). The usefulness of CPP_p as a fluorescent probe is shown in Fig. 8 in which the changes in fluorescence intensities and wavelengths of maximum emission of CPP_p with different solvent systems are illustrated. Changing the solvent system from 70% (V/V) 1,4-dioxane to H_2O resulted in a red shift in the maximum fluorescence emission wavelength from 400 nm to 406 nm with a concommitant increase in the fluorescence intensity (from 49-83) at the emission maxima. This suggests that the fluorescence intensity of CPP_p increases with increased solvent polarity. Fig. 9 shows the emission decay of CPP_p with a fluorescent lifetime of 4.5 nanoseconds upon excitation with nanosecond pulses. The phosphorescence decay of CPP_p is shown in Fig. 10. Equation 1 gives the

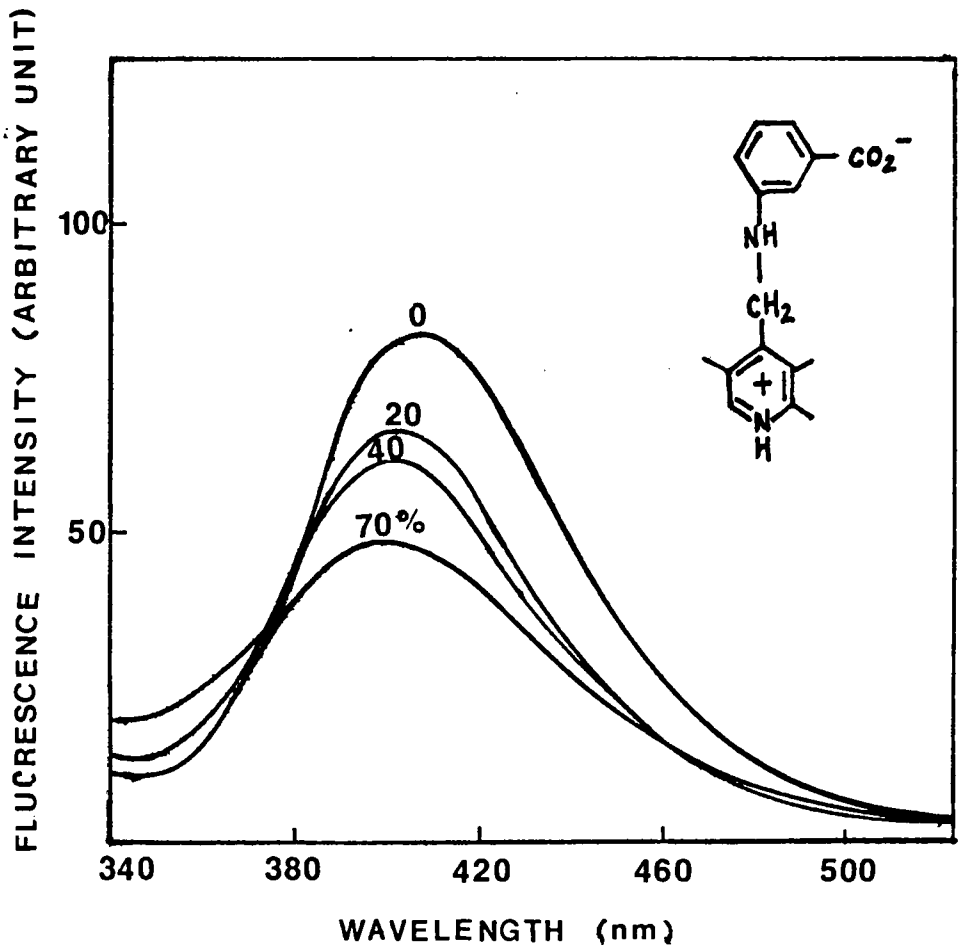

Figure 8. The variation on fluorescence emission spectra for m-carboxyphenyl-pyridoxamine phosphate with changes in solvent composition. The concentration of CPP was 10μM. The percentages of 1,4-dioxane (v/v) in 0.1M potassium phosphate(pH 8.0) are indicated in the curves. Excitation wavelength is at 315 nm.

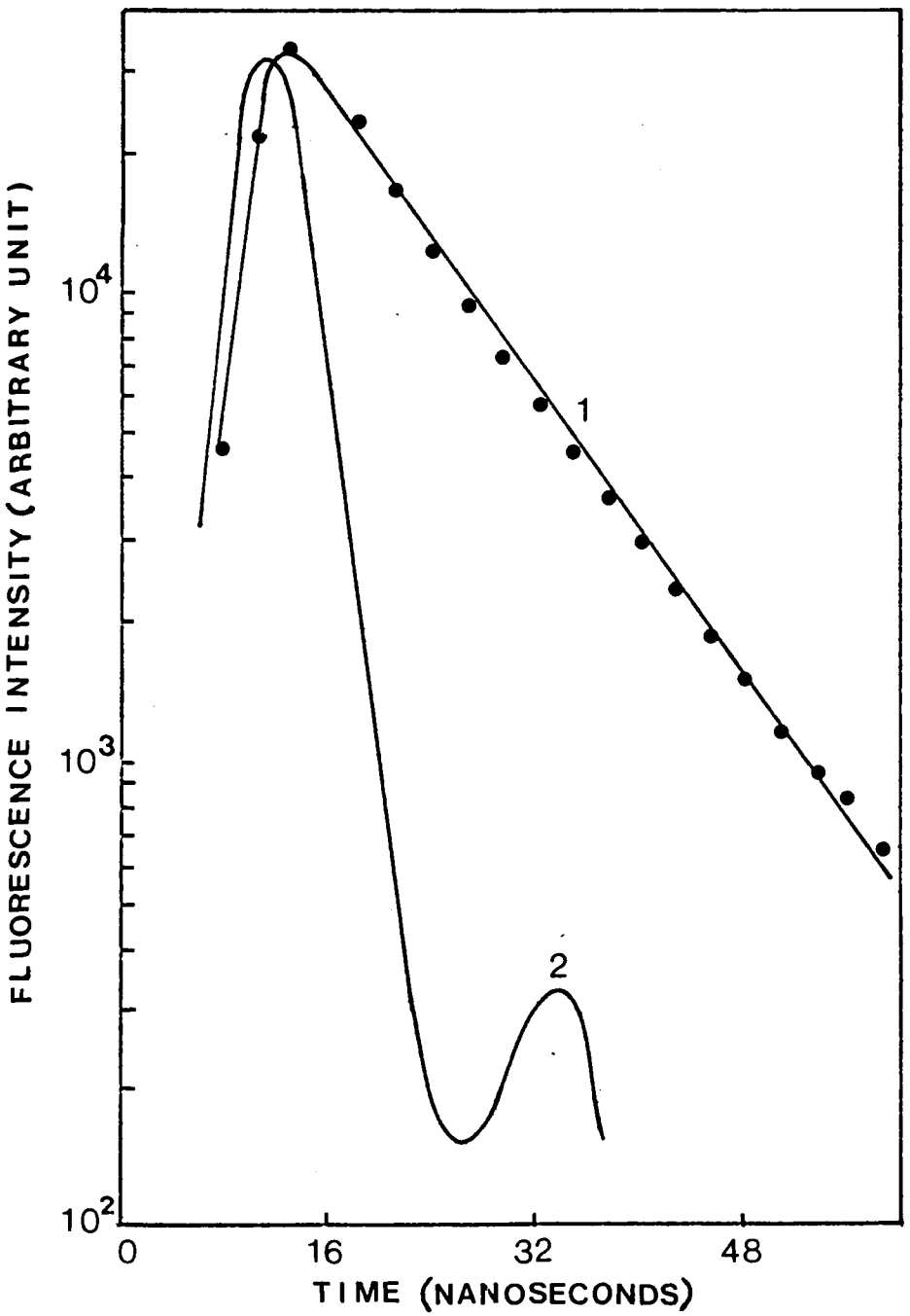

Figure 9. Fluorescence decay of m-carboxyphenyl-pyridoxamine(CPP_p) (1 x 10^{-5}M) in 0.1M potassium buffer (pH 8) obtained with monophotonic fluorescence technique(1). The lamp profile (2) is included in the figure.

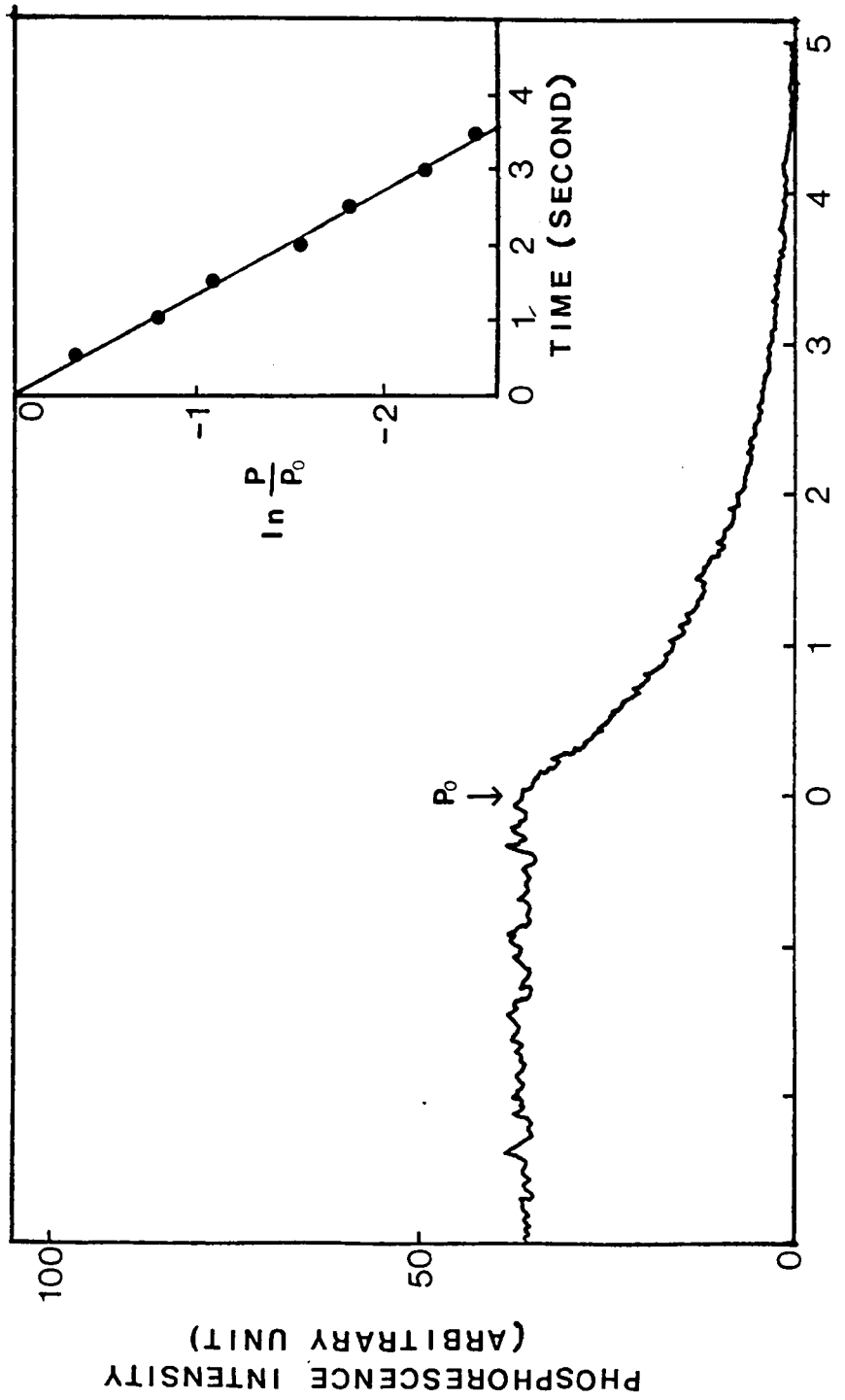

Figure 10. Phosphorescence decay curve of CPP_p(50μM) in ethanol. Excitation wavelength 450 nm. Insert: Plot of ln P/P_o vs. time. The life time of phosphorescence decay obtained for CPP_p was 1.35 ± 0.05 sec.

lifetime in a simple exponential decay:

$$P(t) = P_o \exp(-t/\tau) \qquad (1)$$

where P(t) is the phosphorescence signal at time t. P_o is the phosphorescence at time zero and τ is the phosphorescence decay time. A ln $P(t)/P_o$ vs. t plot gives the phosphorescence decay time. The decay lifetime of CPP_p determined using this method is 1.35 ± 0.05 seconds (Fig. 10).

Since CPP_p is an excellent substrate for PNP oxidase with K_M = 1μM (14), products will be formed immediately following the addition of CPP_p. Therefore, the binding study of CPP_p to the catalytic site of PNP oxidase must be proceeded under the conditions which PNP oxidase does not have the ability for further catalysis after the addition of CPP_p to the enzyme. The addition of CPP_p to the apoPNP oxidase showed a fluorescence enhancement for CPP_p (Fig. 11). This result is different from what was observed for PLPoxime, a strong inhibitor of PNP oxidase. The binding of PLPoxime to the oxidase resulted in a decrease in its fluorescence intensity (Fig. 12). 3-Carboxymethyl FMN is a strong inhibitor of PNP oxidase with K_I = 40nM (12). The addition of 3-carboxymethyl FMN to a mixture containing apoenzyme and substrate was accompanied by a decrease in the fluorescence of the FMN analogue without any effect on the magnitude of the fluorescence emitted by CPP_p (Fig. 11).

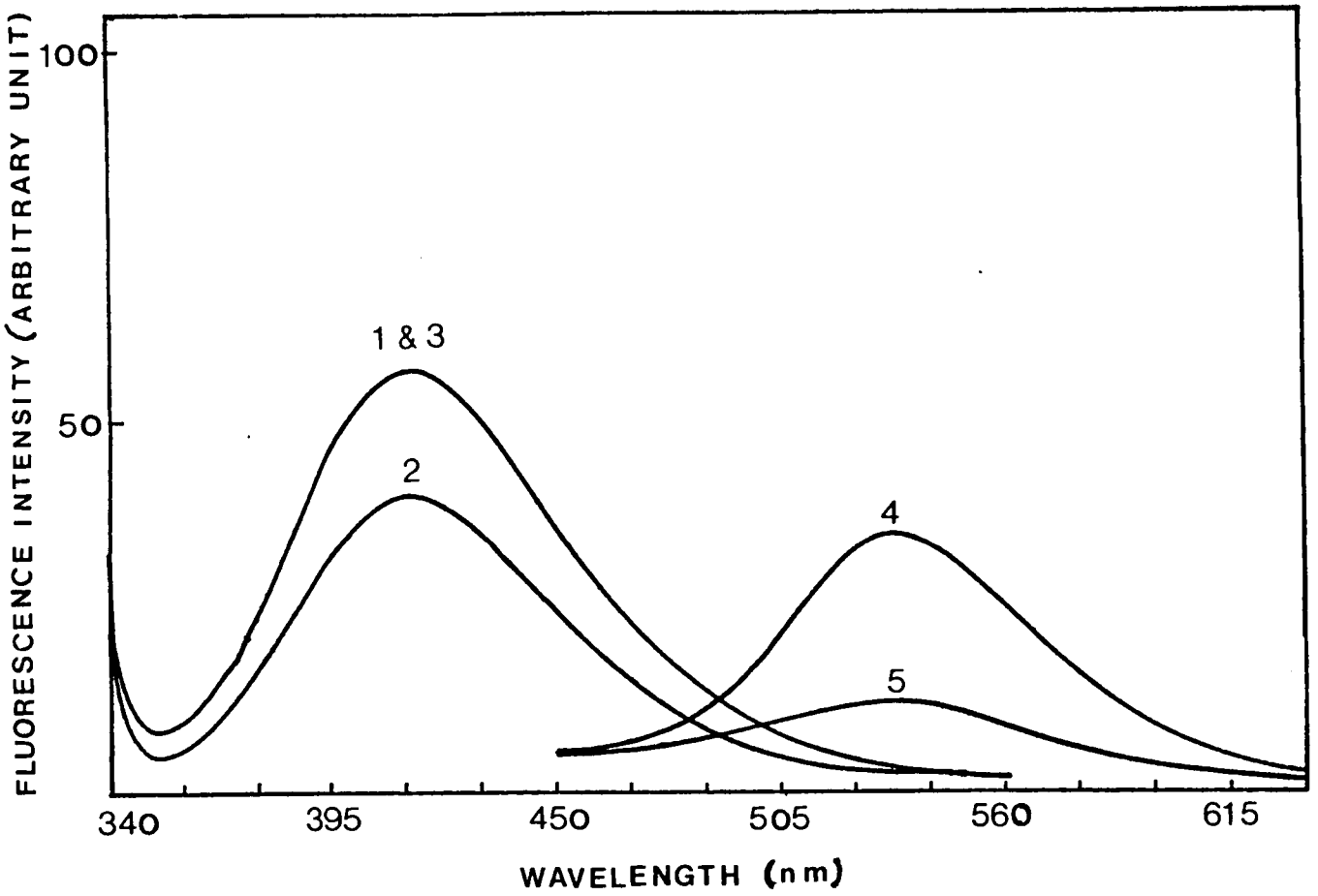

Figure 11. (Curve 1,2,3) Fluorescence spectra of m-carboxyphenyl-pyridoxamine phosphate(10μM) in the presence(1) and absence(2) of apoPNP oxidase(10μM) in 0.1M phosphate buffer(pH 8). Curve 3 is the fluorescence spectum of CPP_p in the presence of apoPNP oxidase and 3-carboxymentyl FMN (10μM). Excitation wavelength 315 nm. (Curve 4,5) Fluorescence spectra of 3-carboxymethyl FMN(10μM) in the absence(4) and presence(5) of apoPNP oxidase(10μM) in 0.1M phosphate buffer(pH 8). Excitation wavelength 380 nm.

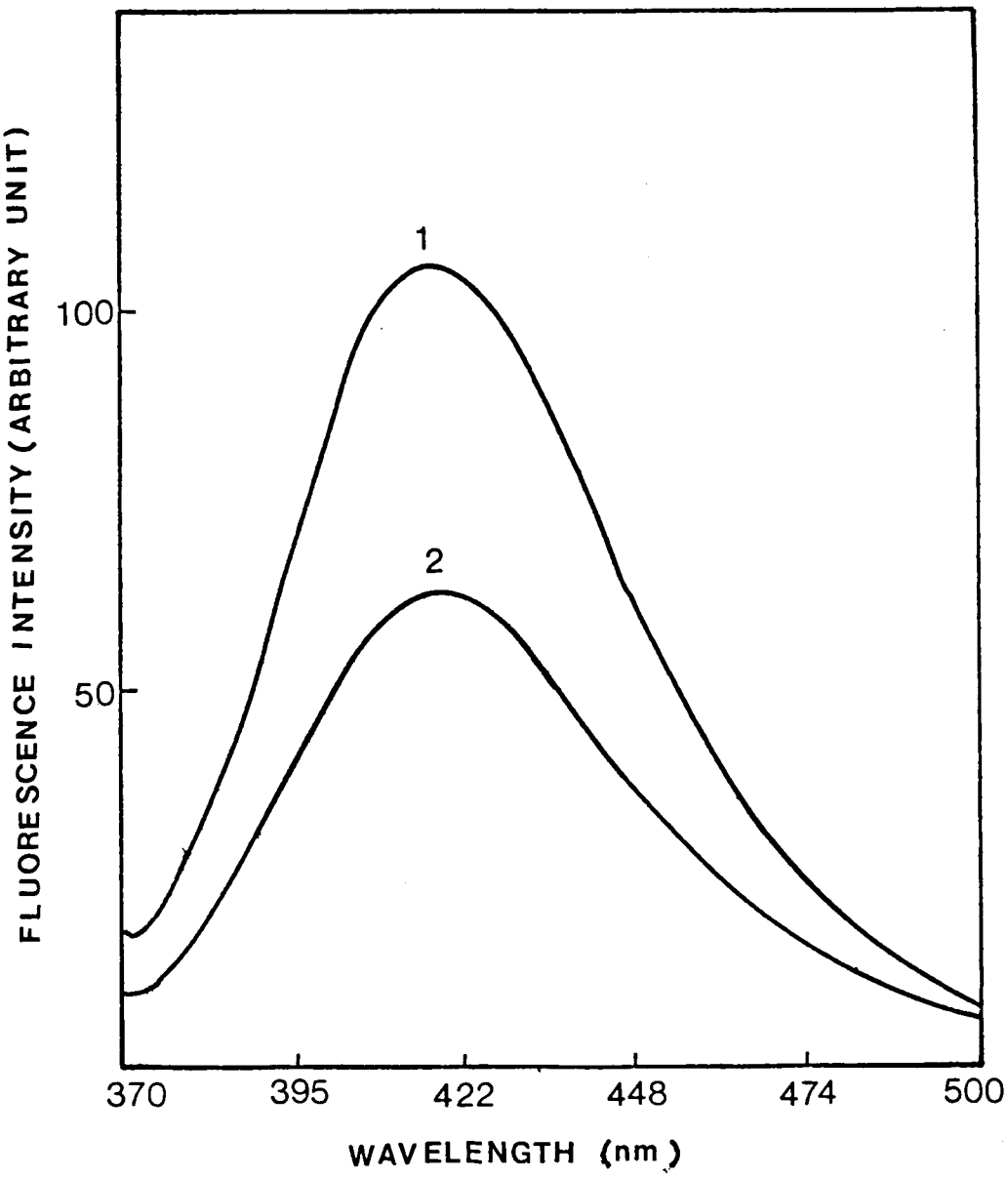

Figure 12. Fluorescence spectra of pyridoxal-5-P oxime(5×10^{-5}M) in the absence(1) and presence(2) of pyridoxine-5-P oxidase(3.6×10^{-5}M) in 0.1M potassium phosphate buffer(pH 8). Excitation wavelength 340 nm.

IV. Discussion

In recent years, the purification of pyridoxine-5-phosphate oxidase from various animal sources and yeast has been reported by several laboratories (8,15,20,21,22). The method in the present work provides a simple and rapid purification procedures compared with those of other groups. This method allows the purification of PNP oxidase to electrophoretic homogenity in five days. The final activity yield of purified oxidase is considerably higher than those of previously reported preparations.

Fluorescence spectroscopy has been proven to be a valuable technique in the study of the active sites of enzymes if a suitable fluorescent chromophore is located near the active center (23). The present studies report the fluorescence properties of m-carboxyphenyl-pyridoxamine phosphate (CPP_p) and the usefulness of the this compound in the binding study to PNP oxidase. It has been reported that CPP_p is an excellent substrate for PNP oxidase with K_M = 1μM (14). Therefore, it is highly selective in terms of its site of attachment to the protein. CPP_p has an absorption and emission spectra distinct from those of aromatic residues of the protein. The results of present studies show that the fluorescence of CPP_p is sensitive to the polarity of the environment and the excited state lifetime of CPP_p is sufficiently long so that the rotational mobility in the active site can be determined. All these

properties suggest that CPP_p can be utilized as a fluorescence probe for the active sites of enzymes.

CPP_p is a stable m-anthranilic acid derivative (24). Before the study of binding of CPP_p to PNP oxidase, it is interesting to study the anthraniloyl residue in the active site of trypsin (see Appendix B).

The fluorescence enhancement detected upon mixing the apoenzyme with CPP_p can be attributed to the binding of this substrate to the enzyme. This result implies that the substrate recognizes its binding site even in the absence of the cofactor FMN. On the other hand, PLPoxime, which is a strong inhibitor of PNP oxidase, showed a fluorescence decrease upon binding to enzyme. It was expected that the same fluorescence change could be observed upon the binding of CPP_p to the catalytic site of PNP oxidase as the result of a dipole-dipole coupling process taken place between this molecule and the FMN analogue bound to the catalytic site. The addition of CPP_p to the apoenzyme showed a fluorescence enhancement in the presence or absence of 3-carboxymethyl-FMN. These results may reflect the different binding orientation of CPP_p and PLPoxime in the catalytic site of PNP oxidase.

In the catalysis process, cofactor FMN of PNP oxidase is reduced and regenerated to the oxidized form by an interaction with molecular oxygen. Therefore, the oxidized form of PNP oxidase can not be regenerated if there is no

oxygen in the reaction mixture. The binding studies of CPP_p to the holoPNP oxidase can proceed if a anaerobic condition can be created. Two alterative methods were tried in order to create anaerobic condition in this preliminary studies (see Appendix C).

LIST OF REFERENCES

LIST OF REFERENCES

1. McCormick, D.B., Gregory, M.E. and Snell, E.E. (1961) J. Biol. Chem. 236, 2076-2082.

2. Neary, J.T. and Diven, W.F. (1970) J. Biol. Chem. 245, 5585-5593.

3. Kwok, F. and Churchich, J.E. (1979) Eur. J. Biochem. 93, 229-235.

4. Spector, R. and Greenwald, L.L. (1978) J. Biol. Chem. 253, 2373-2379.

5. Tiselius, A., Hjerten, S. and Levin, O. (1956) Arch. Biochem. Biophys. 65, 132-136.

6. Kwok, F. and Churchich, J.E. (1979) J. Biol. Chem. 254, 6489-6495.

7. Kallmann and Spruch (1962) Luminescence of organic and inorganic materials. pp. 130.

8. Kwok, F. and Churchich, J. E. (1980) J. Biol. Chem. 255, 882-887.

9. Churchich, J.E., Beeler, T. and Oh K.J. (1975) J. Biol. Chem. 250, 7722-7727

10. Demas, J.N. and Adamson, A.W. (1971) J. Phys. Chem. 75, 2463-2466.

11. Forster, T. (1965) in Modern Quantum Chemistry (Sinanoglu, O. ed.) Part III, pp. 93-137, Academic Press, New York.

12. Merrill, A.H., Kasai, S., Matsui, K., Tsuge, H. and McCormick, D.B. (1979) Biochemistry 18, 3635-3641.

13. Feinstein, R.N. and Lindahl, R. (1973) Anal. Biochem. 56, 353-360.

14. Kim, D.S., Moses, U. and Churchich, J.E. (1981) Eur. J. Biochem. In press.

15. Cash, C.D., Maitre, M., Rumigny, J.F. and Mandel, P. (1980) Biochem. and Biophy. Res. Commu. 96,1755-1760.

16. Davis, B.J. (1964) Ann. N. Y. Acad. Sci. 121, 404-427.

17. Lowry, O.H., Resebrough, N.J., Farr, A.L. and Randall, R.J. (1951) J. Biol. Chem. 193, 265-275.

18. Mayhew, S.G. (1971) Proc. 3rd Int. Symp. Flavins Flavoproteins (Durham. N.C., 1970) pp. 185, University Park Press, Baltimore.

19. Rando, R.R. and Bangerter, F.W. (1977) J. Amer. Chem. Soci. 99, 5141-5145.

20. Wada, H. and Snell, E. (1961) J. Biol. Chem. 236, 2089-2095.

21. McCormick, D.B. and Kazarinoff, M.N. (1975) J. Biol. Chem. 250, 3436-3442.

22. Isuge, H., Ozeki, K., Kiyoko, S.M. and Ohashi, K. (1979) Agric. Biol. Chem. 43, 1801-1807.

23. Steiner, R.F. and Edelhoch, H. (1962) Chem. Rev, 62, 457.

24. Rando, R.R. (1977) Biochemistry, 16, 4604-4610.

25. Haugland, R. P. and Stryer, L. (1967) in Conformation of Biopolymers (Ramachadran, G.N. ed.) Vol. 1. pp. 322-335

26. Churchich, J.E. (1967) Biochem. Biophys. Acta. 147, 511-520.

27. ORR, H., Marshall, J. C., Isenhour, T. L. and Jurs, P. C. (1973) Introduction to Computer Programming for Biological Scientists. pp. 181-186.

APPENDIXES

APPENDIX A

DECONVOLUTION OF FLUORESCENCE DECAY DATA

The aim of this appendix is to describe the computer program that was written based on the demas (10) method for the deconvolution of fluorescence decay data. It is assumed that the user of this program has a computer background on SAS (Statistical Analysis System) which is a computer system consisting of a group of computer programs.

The steps involved in the analysis of true decay curve are summerized below:

1. The program reads in the data, including the number of intervals (N) which was arbitrarily chosen to be 90, the halfwidth (WHALF) of the data sampling interval of the decay trace (in nanoseconds), lamp profile (EX) and experimental fluorescence decay data (EM).

2. The program calculates the W(t) and Z(t) functions, as define in Methods, Section IV, Chapter I, by means of trapozoidal appoximations. The (W.Z) pairs are printed out as (X.Y) pairs.

3. The program plots the lamp profile (EX(t)) and the experimental decay curve (EM(t)).

4. The program plots Z(t) vs. W(t) and shows the relationship between Z and W of the last eighty (Z.W) pairs. Since there is often a very large random fluctuation in the initial values of W(t) and Z(t), the first ten data

pairs are usually ignored for the purposes of this evaluation.

5. PROC CORR in line 55 is used to measure the strength of relationship between two variable W and Z. When the two variables are correlated, there is apparent linear relationship between the values of one and the values of the other.

6. PROC GLM in line 57 is used for regression to generate the equation of the straight line that best fits the points (Z.W) on the graph. The output of GLM gives the estimates for the model parameters-the intercept and the coefficients ($-\tau_F$).

Listing of the program

```
1       DATA DECADE;
2          ARRAY EX(I) EX1-EX90
3          ARRAY EY(I) EY1-EY90
4          ARRAY EM(I) EM1-EM90
5          ARRAY EN(I) EN1-EN90
6          ARRAY SEX(I) SEX1-SEX90
7          ARRAY SEY(I) SEY1-SEY90
8          ARRAY SEM(I) SEM1-SEM90
9          ARRAY SEN(I) SEN1-SEN90
10         ARRAY W(I) W1-W90
11         ARRAY Z(I) Z1-Z90
12         INPUT N WHALF EX1-EX90 EM1-EM90
13         SEX1 = EX1 * WHALF
14         SEM1 = EM1 * WHALF
15         W1 = EM1/SEX1;
16         Z1 = SEM1/SEX1;
17         DO I = 1 TO N;
18            J = I;
19            EY = EX;
20            EN = EM;
21         END;
22         SEY1 =SEX1;
```

```
23          SEN1 = SEM1;
24          DO I = 2 TO N;
25             J = I - 1;
26             SEX = SEY + ( EY+EX) * WHALF;
27             SEM = SEN + ( EN+EM) * WHALF;
28             W = EM/SEX;
29             Z = SEM/SEX;
30             J = J + 1;
31             SEY = SEX;
32             SEN = SEM;
33          END;
34          DO I = 1 TO N;
35             T = I
36             INPUT1 = EX;
37             INPUT2 = EM;
38             X1 = W;
39             Y1 = Z;
40             IF I > 10  THEN
41                DO;
42                   X = W;
43                   Y = Z;
44                END;
45             ELSE;
46             OUTPUT;
47          END;
48          CARDS;
49       PROC PRINT;
50          VAR N WHALF T INPUT1 INPUT2 X1 Y1 X Y;
51       PROC PLOT;
52          PLOT INPUT1*T='*' INPUT2*T='+'/OVERLAY;
53       PROC PLOT;
54          PLOT Y*X='*';
55       PROC CORR;
56          VAR X Y;
57       PROC GLM;
58       MODEL Y = X;
```

APPENDIX B

BINDING OF p-NITROPHENYL ANTHRANILATE TO THE ACTIVE SITE OF TRYPSIN

Materials

p-Nitrophenyl anthranilate (NPA), alchol dehydrogense and trypsin were purchased from Sigma. Acetonitrile was from J. T. Baker Chemical Co.

Methods

Preparation of anthraniloyl trypsin. 1.75 ml of 10^{-2}M p-nitrophenyl anthranilate in acetonitrile was added to 3.5 ml of 2 x 10^{-4}M trypsin in 0.1M phosphate buffer (pH 6.8) at 4°C. The reaction was allowed to proceed at 4°C for 15 hr. The yellow solution was then filtered to remove excess NPA that had precipitated and then dialysed for 2 days against 0.1M phosphate buffer (pH 6.8). Alcohol dehydrogenase was treated exactly the same as trypsin.

Spectroscopy. Fluorescence measurement and evaluation of fluorescence lifetime were the same as described in methods of section IV, Chapter I. Polarization of fluorescence was measured in an instrument previously described by Churchich (26). Illumination was provided by a Xenon-Hg lamp (150 Watts) with wavelengths selected by a quartz prism monochromator. The band-width for exitation was 5 nm. Fluorescence polarized light was

passed through a C-5-3-72 Corning glass filter. The fluorescence polarization (p) is defined as:

$$p = \frac{F_{\parallel} - F_{\perp}}{F_{\parallel} + F_{\perp}}$$

where $F_{\parallel}$ and $F_{\perp}$ are the intensity of emission polarized parallel and perpendicular to the incident light. Absorption spectra were obtained with a Cary spectrophotometer (Model 15).

Results

Spectrophotometric and spectrofluorimetric measurements revealed that p-nitrophenyl anthranilate reacted specifically with trypsin but no reaction took place between alcohol dehydrogenase and NPA (Fig. 13). It has been reported that NPA reacted specifically with the active site of α-chymotrypsin to form a highly fluorescent anthraniloyl chymotrypsin and it seems likely that the anthraniloyl group is esterified to the serine residue in the active site (25).

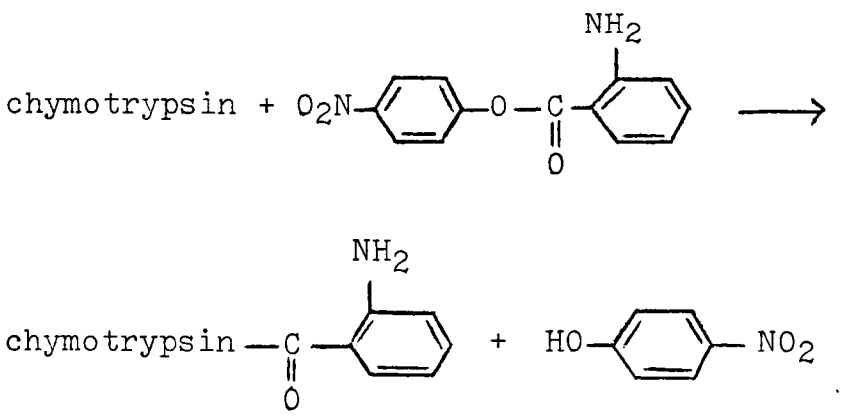

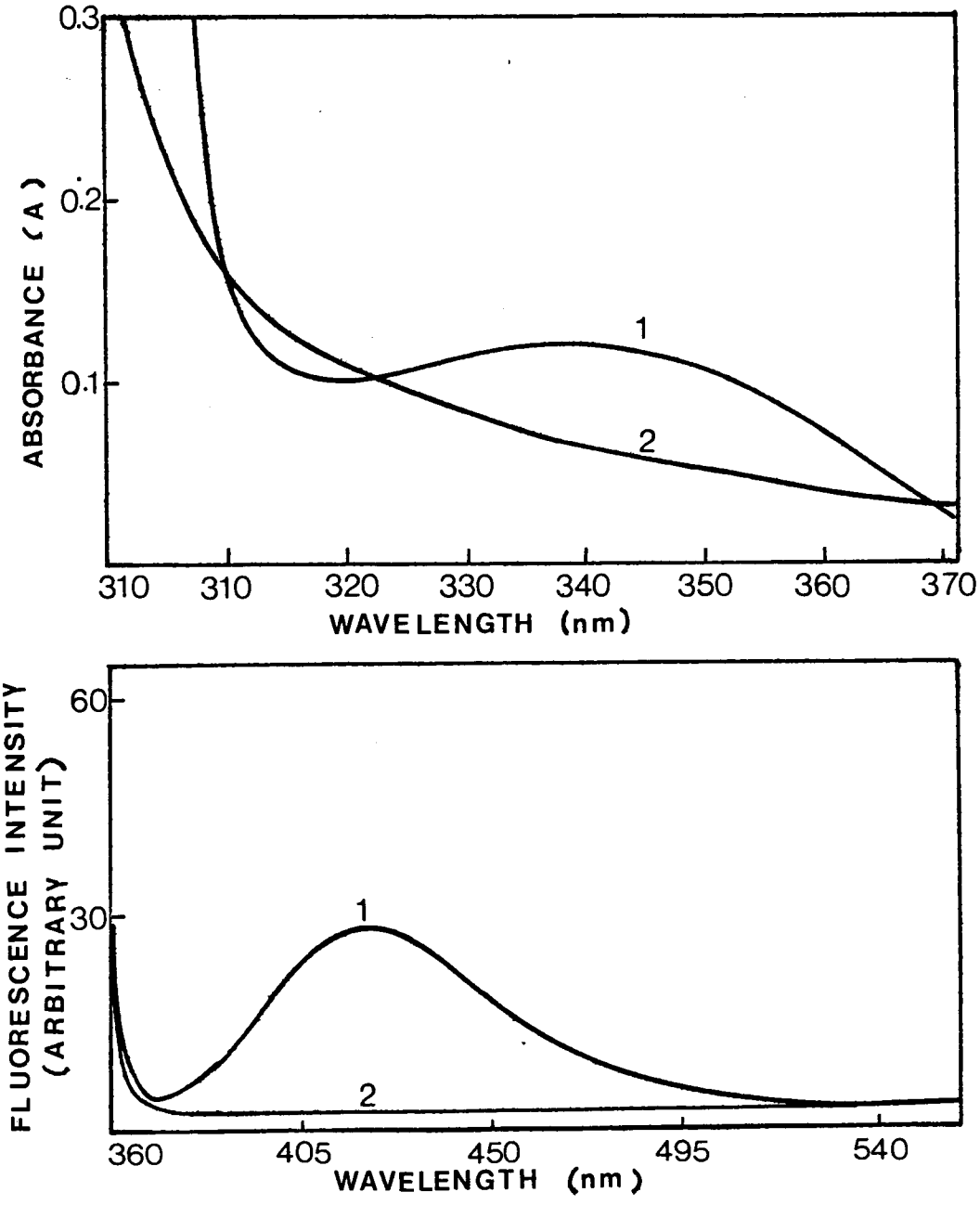

Figure 13. (Upper) Absorption spectra for(1) trypsin and(2) alcohol dehydrogenase(1.3×10^{-4}M for each) reacted with p-nitrophenyl anthranilate(3.3×10^{-3}M). Reaction mixture were dialyzed against 0.1M phosphate buffer(pH 6.8) after reaction were proceeded for 15 hr at 4°C. (Bottom) Emission spectra for(1) trypsin and(2) alcohol dehydrogenase after the same treatment with p-nitrophenyl anthranilate. Excitation wavelength 340 nm.

Similar to chymotrypsin, trypsin contains a serine residue in the active site. Therefore, NPA reacts with the active site of trypsin to form a highly fluorescent anthraniloyl trypsin. This derivative is stable at least two weeks at neutral pH and shows a new absorption peak at 337 nm. Following excitation at 340 nm, NPA shows an emission at 420 nm. The fluorescence polarization of anthraniloyl trypsin was measured in order to determine the rotational relaxation time of the active site. Upon excitation 340 nm, the fluorescence polarization, p, of the derivatized enzyme was 0.215 in 0.1M phosphate buffer, pH 6.8 , at 20°C. The fluorescence polarization (p) was measured at seven different temperatures in the range of 10°C to 30°C. A plot of $1/p - 1/3$ vs. T/η (Fig. 14) gave a straight line which extrapolated to a value of 3.0 at $T/\eta = 0$. This corresponds to a limiting fluorescence polarization, p_o, of 0.30. The rotational relaxation time, ρ, is relate to p, p_o and τ, the excited state lifetime, by the expression:

$$\left(\frac{1}{p} - \frac{1}{3}\right) = \left(\frac{1}{p_o} - \frac{1}{3}\right)\left(1 + \frac{3\tau}{\rho}\right)$$

From nanosecond pulse measurements, a value of 9.1 nsec was obtained for τ. These values give a rotational relaxation time of 41 nsec.

The anthraniloyl trypsin was chosen as a model system in the studies of binding of CPP_p to PNP oxidase

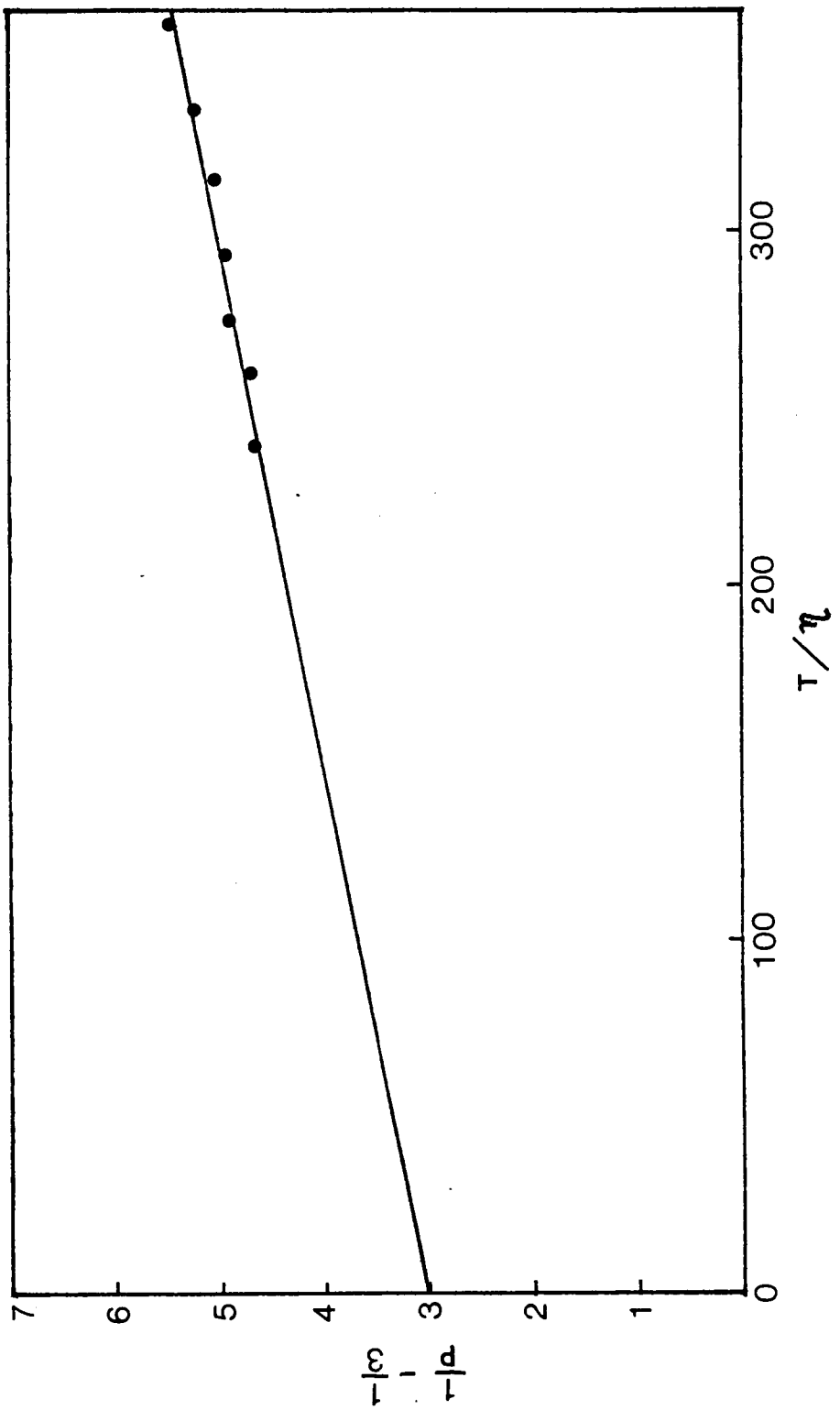

Figure 14. Fluorescence polarization of anthraniloyl trypsin(1.3×10^{-4}M) in 0.1M phosphate buffer(pH 6.8). $1/P - 1/3$ was plot as a function of T/η, to extrapolate to a limiting fluorescence polarization, P_o, at $T/\eta = 0$.

also due to the derivative is stable for a long period of time at neutral pH, allowing a detailed study of its spectroscopic properties. Absorption and fluorescence studies of anthraniloyl trypsin can also provide a measure of the rotational mobility of the active site of the acyl enzyme. Rotational relaxation time, ρ = 41 nsec, suggests that anthraniloyl chromophore has no rotational mobility independent of the motion of the whole trypsin molecule. Spectrophotometric and spectrofluorimetric measurement also revealed that anthraniloyl residue was covalent bound to trypsin. Therefore, from the studies of this model system, one can get some informations about the fluorescence properties of anthraniloyl residue which is covalently bound to the protein.

APPENDIX C

ANAEROBIC CONDITION FOR THE STUDYING OF BINDING OF CPP_p TO PNP OXIDASE

Anaerobic condition was created in an anaerobic fluorescence cuvette which contained two side chambers at the top of cuvette. After introducing nitrogen gas into the solution for 5 min, the cuvette was sealed. The different components in the cuvette and side chambers could be mixed after the oxygen in the solution was displaced. An alternative method to create an anaerobic condition was using Glucose oxidase (GOD). In the presence of excess amount of GOD and glucose, the oxygen in the enzyme solution and substrate solutions was consumed and thereby creating an anaerobic condition. The consumption of oxygen in the solution was monitored by an Aminco DW 2 double-beam spectrophotometer with a vibrating platinum electrode assembly using an open cuvette.

It has been reported that biacetyl has a fluorescence maximum at 469 nm(7). The phosphorescence of biacetyl at 513 nm can only be observed in the absence of oxygen. By virtue of the high yield of intersystem crossing to the lowest triplet state of biacetyl, phosphorescence is observed (7). Fig. 15 shows the appearance of emission peak after the introduction of nitrogen gas into the biacetyl solution for 5 min. This result suggests that one

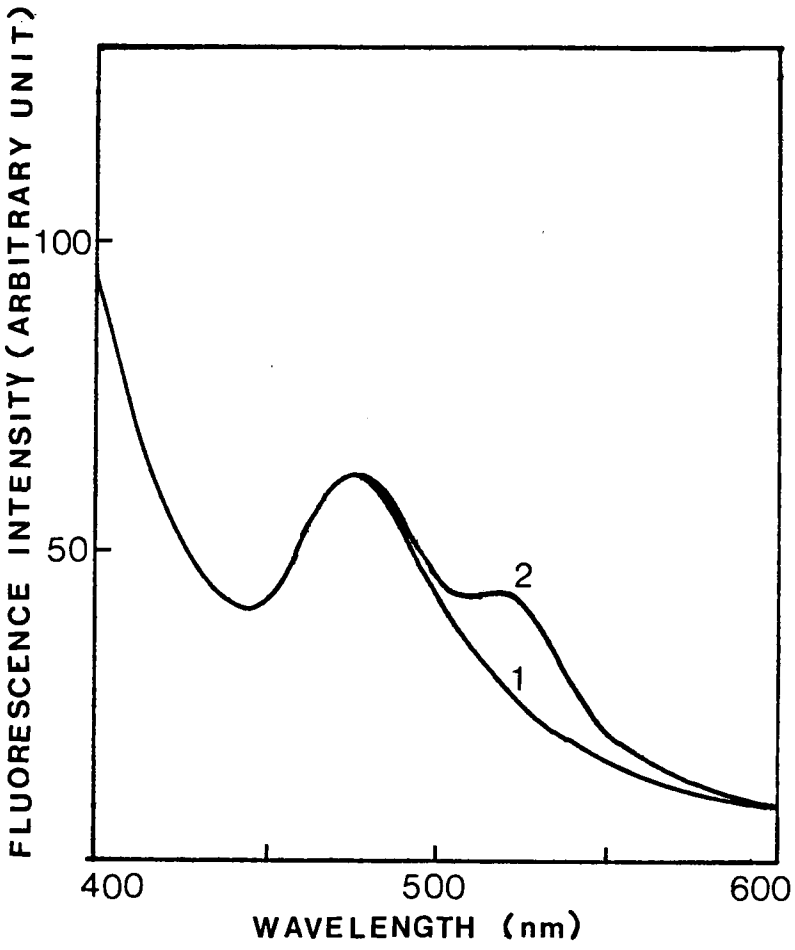

Figure 15. Emission spectra of biacetyl in cyclohexane before(1) and after(2) replacing the oxygen with nitrogen for 5 min. Excitation vavelength 360 nm.

can obtain a anaerobic condition in the fluorescence cuvette. Fig. 16 shows that the anaerobic condition can also be obtained in the presence of GOD and glucose. GOD catalyzes the oxidation of glucose and removes the oxygen from the solution. The products of GOD, gluconolactone and H_2O_2, have no effect on the activity of PNP oxidase. Therefore, it is a good system to use to obtain anaerobic condition in our studies. Different concentrations of GOD were investigated in an attempt to find out an optimum concentration to use to create the anaerobic condition. As shown in Fig. 16, 50λ of GOD (1mg/ml) in 2 ml solution could almost consume all the oxygen in the solution. The gradually increasing concentration of oxygen later might be due to the back diffusion of oxygen into the reaction mixture.

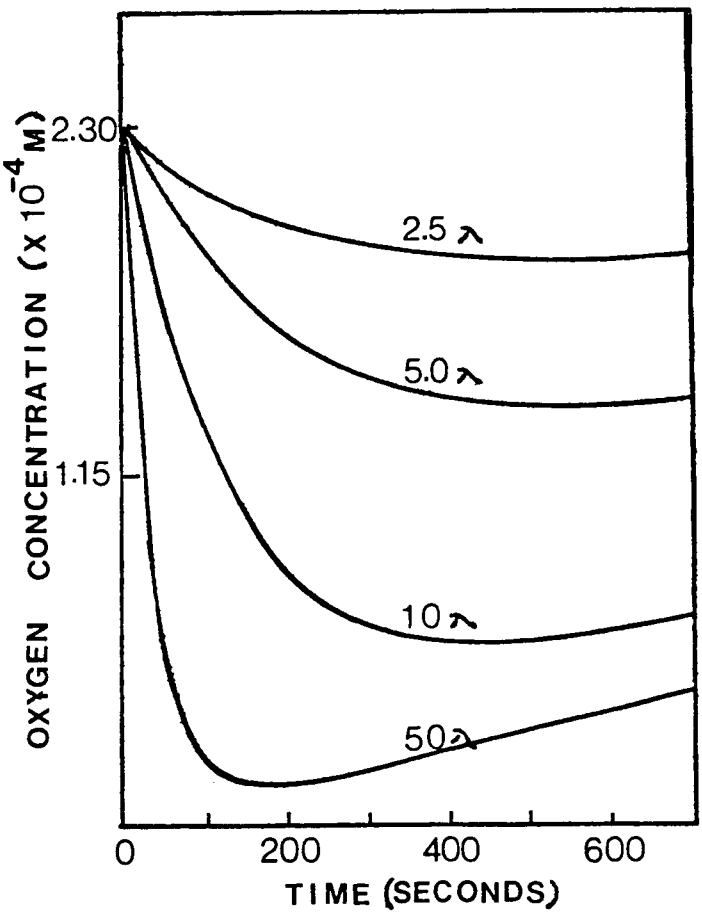

Figure 16. Oxygen consumption in the presence of glucose oxidase and glucose. As indicated in the graph: 2.5, 5.0, 10, or 50 Å of glucose oxidase(1mg/ml) was added to 2 ml of 0.1M potassium buffer(pH 8) containing 50 mM glucose. Initial concentration of oxygen in the solution, 2.3×10^{-4}M, was obtained from the literature.

VITA

Christine Hshiao-Mean Wu was born July 30,1955, in Taiwan, Republic of China. She graduated from Chung-Shan Senior High School for girls, Taipei, Taiwan in 1973. She then attended Fu-Jen Catholic University, Taiwan, and received a Bachelor of Science degree majoring in Biology in 1977. Miss Wu was then employed as a research assistant by the Department of Biomorphics, National Defense Medical Center, Taiwan, for one year. In September 1978, she came to United States and started her graduate study at the University of Tennessee at Koxville. During her tenure at this institution she was supported by a teaching assistantship in the Biochemistry Department and received her Master of Science degree in Biochemistry in June 1981.